

Supporting Information

Uranyl-silicotungstate containing hybrid building units $\{\alpha\text{-SiW}_9\}$ and $\{\gamma\text{-SiW}_{10}\}$ with excellent catalytic activities in the three-component synthesis of dihydropyrimidin-2(1*H*)-ones

Jian-Hua Ding,^{‡*a*} Yu-Feng Liu,^{‡*a*} Zhao-Teng Tian,^{*a*} Pei-Jie Lin,^{*a*} Feng Yang,^{*c*} Ke Li,^{**a*} Guo-Ping Yang^{**a,b*}, and Yong-Ge Wei^{**b*}

^{*a*} School of Chemistry, Biology and Material Science, Jiangxi Province Key Laboratory of Synthetic Chemistry, Jiangxi Key Laboratory for Mass Spectrometry and Instrumentation, East China University of Technology, Nanchang 330013, China.

^{*b*} Key Lab of Organic Optoelectronics & Molecular Engineering of Ministry of Education, Department of Chemistry, Tsinghua University, Beijing 100084, China.

^{*c*} School of Chemistry and Pharmaceutical Sciences, Guangxi Normal University, Guilin, 541000, China.

‡ Contributed equally to this work.

Table of Contents

1. General Information	2
2. Experimental.....	2
3. Characterization of \mathbf{U}_3	3
4. Characterization of Products	11
5. NMR Spectra	16
6. References	31

1. General Information

Materials and Methods

$K_8[\gamma\text{-SiW}_{10}\text{O}_{36}]\cdot12\text{H}_2\text{O}$ was prepared according to the reported method.¹ Other reagents were all obtained from commercial sources and used without further purification. *CAUTION! Appropriate precautions are essential for handling all uranium compounds.*

Electrospray ionization mass spectrum (ESI-MS) data were obtained on a Bruker Autoflex maX matrix-assisted laser desorption ionization-time of flight (MALDI-TOF) mass spectrometer in negative mode with a concentration of 10^{-3} mol/L in water. The FT-IR spectrum was obtained by using a Fourier transform infrared (FT-IR) (4000-500 cm^{-1}) spectrometer (Thermo Nicolet iS5) at 0.5 cm^{-1} resolution and 16 scans. Raman spectra were performed on an RM5 spectrometer (Edinburgh Instrument) from 1200-100 cm^{-1} . Solid-state luminescence data were acquired at room temperature on a steady-state spectrometer (FLS-980, Edinburgh) with a 450 W xenon lamp. Thermogravimetric analyses (TGA) were performed under air atmosphere on Mettler-Toledo TGA/SDTA 851^e thermal analyzer from 25 to 1000 °C. Inductively coupled plasma optical emission spectrum (ICP-OES) data were obtained on an Agilent 725 ICP-OES spectrometer. The scanning electron microscope (SEM) and energy dispersive spectroscopy (EDS) maps were collected on an FEI Nova NanoSEM 450 field emission scanning electron microscope equipping an Oxford X-Max 20 EDS. The ^1H and ^{13}C spectra were recorded on a Brucker ADVANCE III spectrometer at 500 MHz and 126 MHz, and chemical shifts were reported in parts per million (ppm). Flash column chromatography was performed using silica gel of 200-300 mesh. The GC analysis was performed on Agilent 7890B equipped with a capillary column (HP-5, 30 m × 0.25 μm) using a flame ionization detector.

X-ray Crystallography

The single crystal X-ray diffraction data were collected on Bruker D8 Smart Apex II diffractometer with graphite monochromated Mo K α radiation ($\lambda = 0.71073 \text{ \AA}$). Intensities were collected by ω -scan and reduced on *APEX 3* and a multi-scan absorption correction was applied.² The structures were solved and refined on the *Olex2* using the *SHELX* package after being handled with the *SQUEEZE* procedure in *PLATON*.³ Parameters of the crystal data collection and refinement are given in Table S1. Selected bond lengths (\AA), angles (°), and weak coordination interactions are given in Table S2 and S3, respectively. The CSD number of \mathbf{U}_3 is 2132862.

2. Experimental

Synthesis of \mathbf{U}_3

To a NaCl aqueous solution (0.25 M, 20 mL), $\text{UO}_2(\text{OAc})_2\cdot2\text{H}_2\text{O}$ (0.1 mmol, 0.0424 g) and $K_8[\gamma\text{-SiW}_{10}\text{O}_{36}]\cdot12\text{H}_2\text{O}$ (0.4 mmol, 1.1884 g) were dissolved successively. The pH value of the mixture was then adjusted to 5.9 using 1 M HCl. The cloudy solution was heated and stirred at 85 °C for 30 min. During the heating procedure, this cloudy solution would transform from cloudy to clear and then cloudy again. NaCl (4 g) was then added to the solution and stirred for 5 min. The resulting hot solution was filtered and the filtrate was left to evaporate at room temperature. A cold room temperature (below 10°C) is necessary for the formation of \mathbf{U}_3 . Unknown and cube crystals will appear if the room temperature is higher.⁴ Yellow-green crystals of \mathbf{U}_3 with rodlike shapes were collected after two weeks (yield: 11% based on $\text{UO}_2(\text{OAc})_2\cdot2\text{H}_2\text{O}$).

Typical procedure of dehydration condensation reaction catalyzed by \mathbf{U}_3

Benzaldehyde (1 mmol), ethyl acetoacetate (1.5 mmol), urea (1 mmol), and \mathbf{U}_3 (0.2 mol %) were added to a 4 mL reaction vial. The reaction was carried out at 100 °C for 3 h. After cooling to room temperature, the crude was

dissolved in hot EtOH (10 mL). After simple filtration, the filtrate was cooled in an ice bath to promote the recrystallization of the desired product.

3. Characterization of \mathbf{U}_3

Table S1. Crystallographic data and structure refinement of \mathbf{U}_3 (SQUEEZE)

CSD No.	2132862
Empirical formula	$\text{H}_{52}\text{K}_6\text{Na}_9\text{O}_{174}\text{Si}_4\text{U}_3\text{W}_{39}$
Fw	11274.52
T/K	150.0
Crystal system	triclinic
Space group	<i>P</i> -1
<i>a</i> /Å	23.237(3)
<i>b</i> /Å	23.923(2)
<i>c</i> /Å	23.994(2)
α (°)	60.314(3)
β (°)	72.031(3)
γ (°)	83.497(3)
<i>V</i> /Å ³	11009.9(19)
<i>F</i> (000)	9750.0
<i>Z</i>	2
ρ_{calcd} (g·cm ⁻³)	3.401
μ (mm ⁻¹)	22.717
Reflections collected	167903
Unique reflections	54741 ($R_{\text{int}} = 0.1468$)
Parameter	2206
GOOF on F^2	1.037
R_1^{a} [$I \geq 2\sigma(I)$]	0.0837
wR_2^{b} (all data)	0.2461

$$^{\text{a}}R_1 = \sum ||F_o| - |F_c|| / \sum |F_o|, ^{\text{b}}wR_2 = \{\sum [w(F_o^2 - F_c^2)^2] / \sum [w(F_o^2)^2]\}^{1/2}$$

Table S2. Selected bond lengths (\AA) and angles ($^\circ$) in \mathbf{U}_3 .

U1-O1	1.801(16)	K1-O12	2.878(17)
U1-O2	1.736(16)	K1-O17	2.775(17)
U1-O7	2.52(2)	K1-O18	2.808(18)
U1-O10	2.359(17)	K1-O47	2.836(17)
U1-O11	2.383(18)	K1-O49	2.870(18)
U1-O16	2.339(18)	K1-O151	2.78(2)
U1-O17	2.338(18)	K2-O14	2.868(19)
U2-O3	1.795(18)	K2-O19	2.766(19)
U2-O4	1.794(18)	K2-O20	2.741(17)
U2-O8	2.498(19)	K2-O77	2.898(17)
U2-O12	2.346(17)	K2-O152	2.76(2)
U2-O13	2.355(17)	K3-O11	2.847(17)
U2-O18	2.304(17)	K3-O16	2.789(18)
U2-O19	2.337(17)	K3-O21	2.786(17)
U3-O5	1.811(17)	K3-O103	2.892(19)
U3-O6	1.781(17)	K3-O104	2.873(17)
U3-O9	2.462(18)	K3-O153	2.77(2)
U3-O14	2.361(16)	K4-O1	2.898(18)
U3-O15	2.368(16)	K4-O5	2.899(19)
U3-O20	2.290(17)	O1-U1-O2	178.0(9)
U3-O21	2.294(17)	O3-U2-O4	179.4(7)
K1-O10	2.838(16)	O5-U3-O6	179.0(8)

Table S3. Selected distances of the weak coordination interactions (\AA) for K(I) ions in \mathbf{U}_3 .

K1···O1	3.095(18)	K3···O5	3.193(16)
K1···O3	3.115(17)	K3···O15	2.916(18)
K1···O23	2.975(19)	K3···O27	2.969(19)
K2···O3	3.218(18)	K4···O3	2.92(2)
K2···O5	3.134(17)	K4···O151	3.277(19)
K2···O13	2.929(18)	K4···O152	2.935(18)
K2···O25	2.979(19)	K4···O153	2.92(2)
K2···O75	2.922(17)	K4···O154	2.92(4)
K3···O1	3.216(18)	K4···O155	3.00(4)

Table S4. Hydrogen bonds in \mathbf{U}_3 .

D-H···A	d(D-H)/Å	d(H···A)/Å	d(D···A)/Å	\angle (DHA)/°
O7-H7A···O145	0.94	1.90	2.68(3)	138.7
O7-H7B···O150	0.94	1.80	2.71(3)	162.4
O8-H8A···O147	0.92	1.92	2.79(3)	157.1
O8-H8B···O146	0.92	1.91	2.70(3)	143.2
O9-H9A···O149	0.88	1.99	2.76(3)	145.6
O9-H9A···O148	0.88	1.90	2.67(3)	144.7
O151-H15A···O145	0.99	2.05	3.03(3)	170.9
O151-H15B···O146	0.99	2.14	3.13(3)	177.1
O152-H15C···O147	0.99	2.11	3.10(3)	171.7
O152-H15D···O148	0.99	2.18	3.17(3)	174.5
O153-H15E···O149	0.99	2.12	3.11(3)	172.8
O153-H15F···O150	0.99	2.09	3.08(3)	174.4

Table S5. Bond valence calculations for U atoms.

Atom	Bond Valence Sum	Valence State
U1	6.778	+6
U2	6.568	+6
U3	6.633	+6

Bond valence sum (BVS) analysis: The BVS values (V_i) of U atoms in \mathbf{U}_3 were calculated using the following equation:⁵

$$V_i = \Sigma \exp[(r_0 - r_{ij})/B] \quad (1)$$

where r_0 is the bond valence parameter for a given atom pair, r_{ij} is the bond length between atoms i and j obtained from the crystal structure, and B is a constant with the value 0.37 Å.

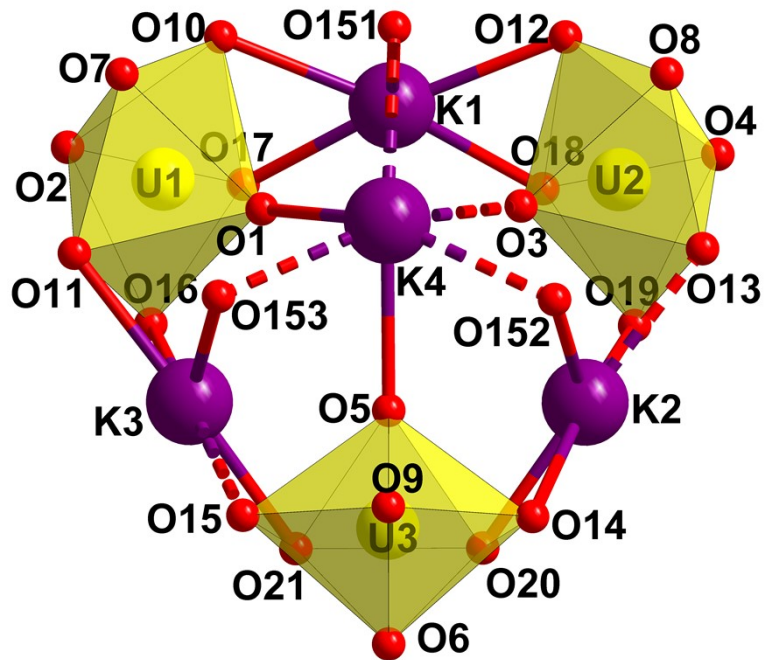


Fig. S1 The coordination environment of the $\{K_4(UO_2)_3(H_2O)_6\}$ chromophore in \mathbf{U}_3 .

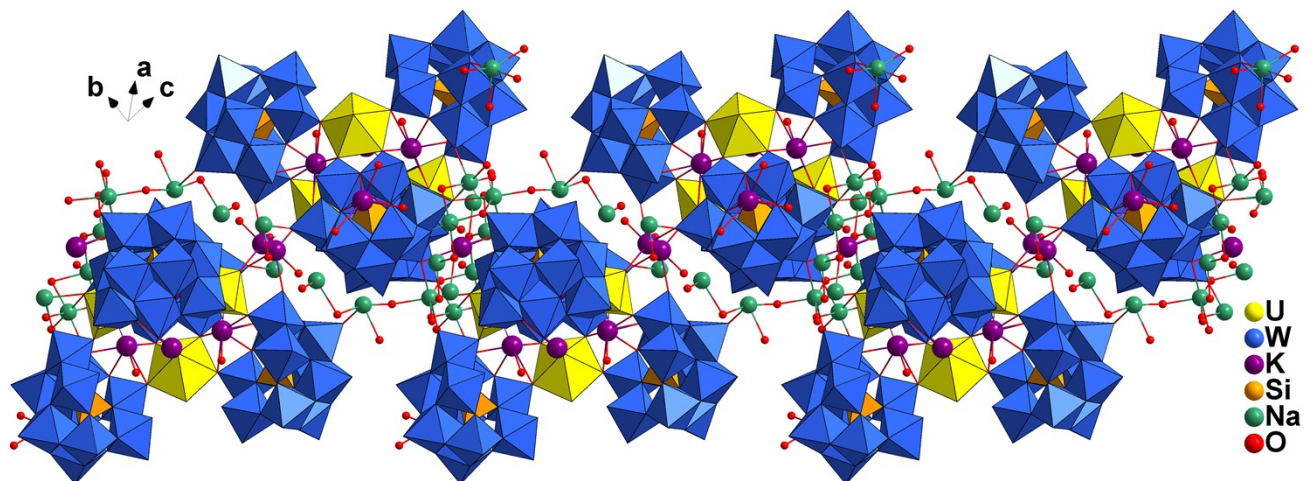


Fig. S2 View of the 1D chain in \mathbf{U}_3 .

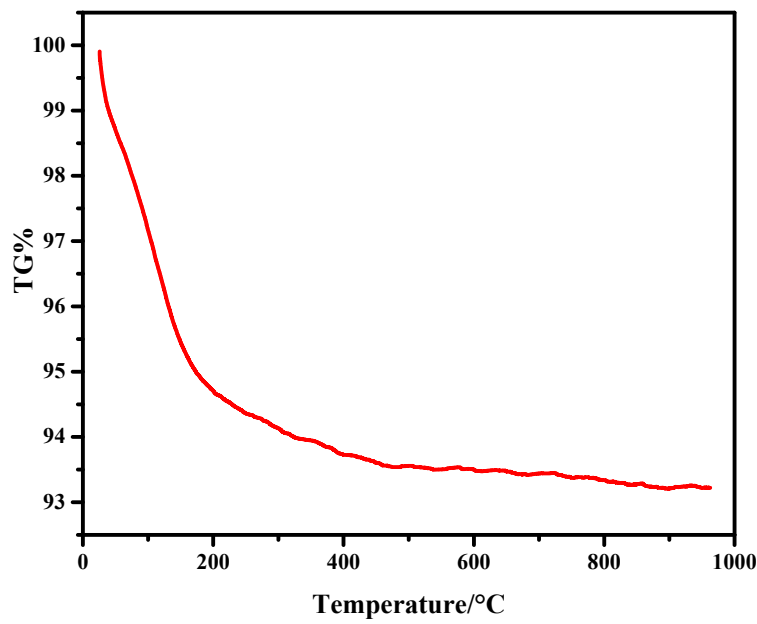


Fig. S3 TGA curve of U_3 .

The TGA curve of U_3 gives a 5.86% weight loss from room temperature to 300 °C, which is corresponding to 42 water molecules. Thus, the number of lattice water molecules removed by SQUEEZE is 16.

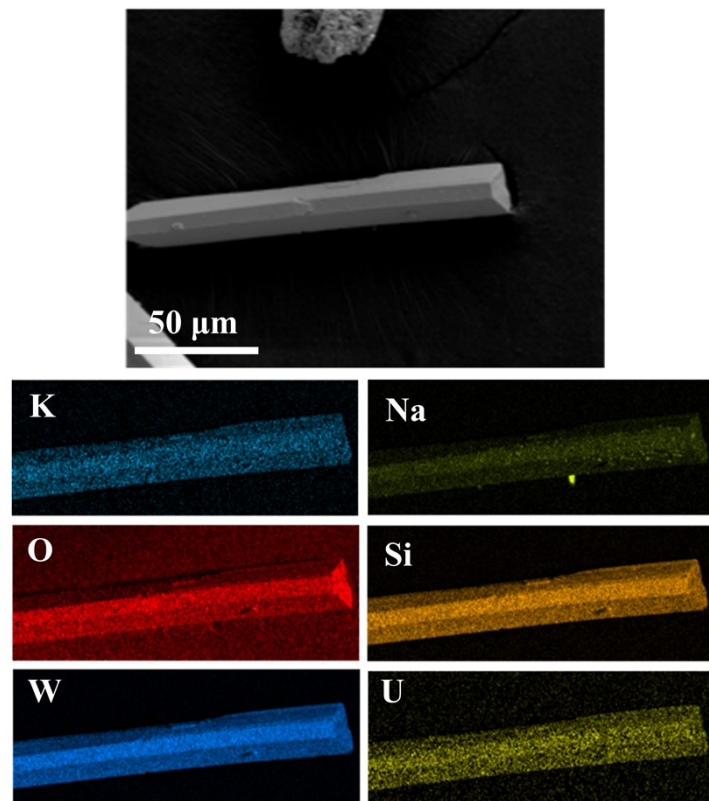


Fig. S4 EDS mapping of U_3 .

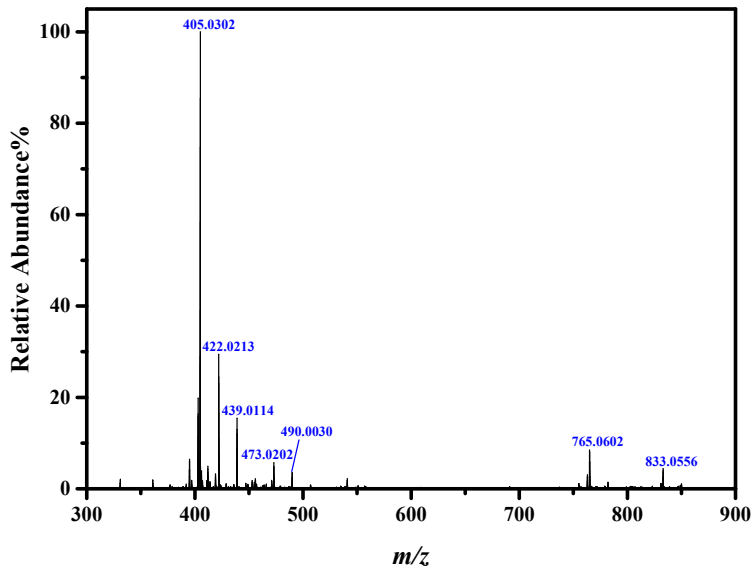


Fig. S5 ESI-MS of \mathbf{U}_3 .

Table S6. Assignment of peaks for \mathbf{U}_3 .

Identification	Charge	Measured m/z	Simulated m/z
$[\text{NaK}_3(\text{H}_2\text{O})_{32}(\text{UO}_2)(\text{SiW}_9\text{O}_{34})(\text{SiW}_{10}\text{O}_{36})_2]^{20-}$	-20	405.0302	405.0109
$[\text{H}_3\text{NaK}_2(\text{H}_2\text{O})_6(\text{UO}_2)(\text{SiW}_9\text{O}_{34})(\text{SiW}_{10}\text{O}_{36})_2]^{18-}$	-18	422.0213	422.0002
$[\text{NaK}_3(\text{H}_2\text{O})_6(\text{UO}_2)_2(\text{SiW}_9\text{O}_{34})(\text{SiW}_{10}\text{O}_{36})_2]^{18-}$	-18	439.0114	438.9991
$[\text{H}_3\text{K}_2(\text{H}_2\text{O})_{17}(\text{UO}_2)_2(\text{SiW}_9\text{O}_{34})(\text{SiW}_{10}\text{O}_{36})_2]^{17-}$	-17	473.0202	473.0101
$\{\text{K}_2(\text{H}_2\text{O})_4[\text{K}_4(\text{UO}_2)_3(\text{H}_2\text{O})_6(\text{SiW}_9\text{O}_{34})(\text{SiW}_{10}\text{O}_{36})_3]\}^{22-}$	-22	490.0030/490.0158	490.0577
$\{\text{HNa}_5\text{K}_3(\text{H}_2\text{O})_{34}[\text{K}_4(\text{UO}_2)_3(\text{H}_2\text{O})_6(\text{SiW}_9\text{O}_{34})(\text{SiW}_{10}\text{O}_{36})_3]\}^{15-}$	-15	765.0602	765.1007
$\{\text{H}_7\text{K}_4(\text{H}_2\text{O})_2[\text{K}_4(\text{UO}_2)_3(\text{H}_2\text{O})_6(\text{SiW}_9\text{O}_{34})(\text{SiW}_{10}\text{O}_{36})_3]\}^{13-}$	-13	833.0556	833.0950

The chemical behaviors of \mathbf{U}_3 in water were evaluated using the electrospray ionization mass spectrum (ESI-MS) (Fig. S3 and Table S6). Unfortunately, the polyanion of $[\text{K}_4(\text{UO}_2)_3(\text{H}_2\text{O})_6(\alpha\text{-SiW}_9\text{O}_{34})(\gamma\text{-SiW}_{10}\text{O}_{36})_3]^{24-}$ was not found and the main four peaks (m/z 405.0302, 422.0213, 439.0114, and 473.0202) were all assigned to be the decomposition products of $[\text{K}_4(\text{UO}_2)_3(\text{H}_2\text{O})_6(\alpha\text{-SiW}_9\text{O}_{34})(\gamma\text{-SiW}_{10}\text{O}_{36})_3]^{24-}$. The unsaturated coordination structure may be responsible for the decomposition of $[\text{K}_4(\text{UO}_2)_3(\text{H}_2\text{O})_6(\alpha\text{-SiW}_9\text{O}_{34})(\gamma\text{-SiW}_{10}\text{O}_{36})_3]^{24-}$ in electrospray ionization. But the rest four peaks (m/z 490.0030/490.0158, 765.0602, and 833.0556) were assigned to be the product of $[\text{K}_4(\text{UO}_2)_3(\text{H}_2\text{O})_6(\alpha\text{-SiW}_9\text{O}_{34})(\gamma\text{-SiW}_{10}\text{O}_{36})_3]^{24-}$ combining different ions and water molecules.

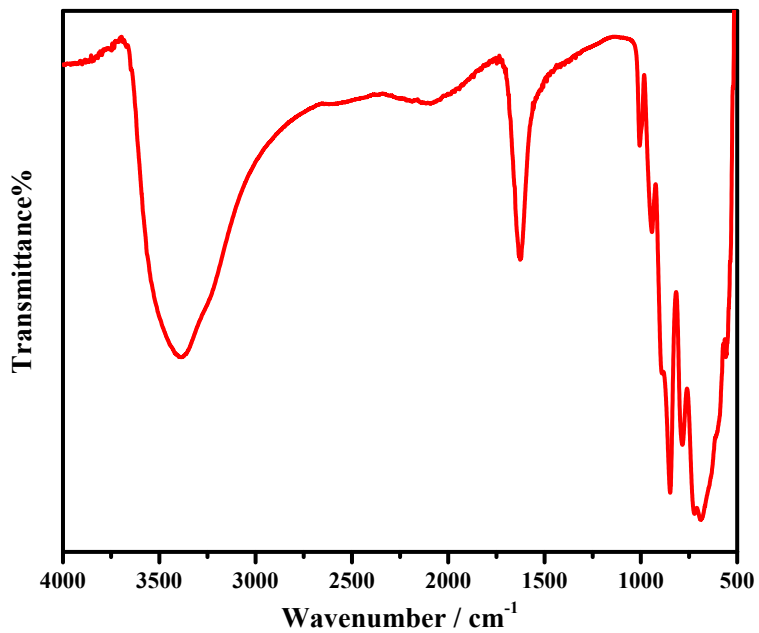


Fig. S7 FT-IR spectrum of \mathbf{U}_3 .

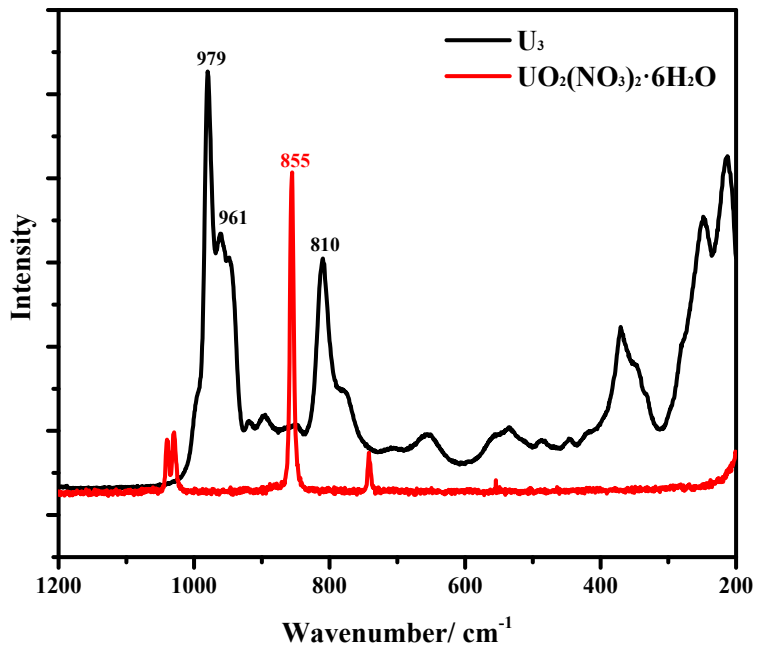


Fig. S8 Raman spectra of \mathbf{U}_3 and $\text{UO}_2(\text{NO}_3)_2 \cdot 6\text{H}_2\text{O}$.

The Raman spectra of \mathbf{U}_3 and solid $\text{UO}_2(\text{NO}_3)_2 \cdot 6\text{H}_2\text{O}$ are shown in Fig. S5. The band at 810 cm⁻¹ is similar to the reported Raman bands of O=U=O which can be attributed to the *trans*-related O=U=O symmetric stretching vibration.⁶ The lower wavenumber suggests the weaker O=U=O bonds in the $[\text{K}_4(\text{UO}_2)_3(\text{H}_2\text{O})_6(\alpha\text{-SiW}_9\text{O}_{34})(\gamma\text{-SiW}_{10}\text{O}_{36})]^{24-}$ polyanion compared with aqueous $\text{UO}_2(\text{NO}_3)_2$ (870 cm⁻¹) and solid $\text{UO}_2(\text{NO}_3)_2$ (855 cm⁻¹).⁷ The weak coordination interactions of U=O \cdots K may weaken the U=O bonds and cause the shift of the corresponding band. The strong band at 979 and 961 cm⁻¹ may be attributed to the symmetric stretching mode of $\nu(\text{W}=\text{O}_d)$ in $\{\gamma$ -

$\text{SiW}_{10}\}$ and $\{\alpha\text{-SiW}_9\}$, respectively.

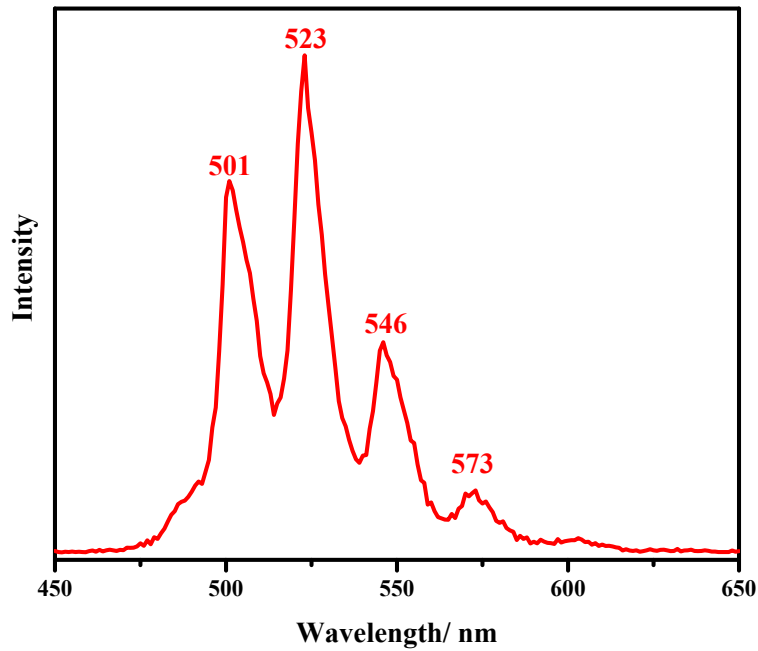
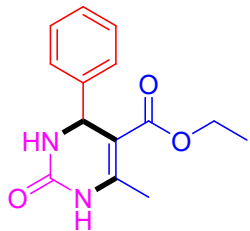


Fig. S9 Solid-state luminescence spectrum of \mathbf{U}_3 , excitation wavelength 353 nm.

The solid-state luminescence spectrum of \mathbf{U}_3 shows similar mountain-like peaks as the two reported U-POWs.⁸ When the excitation wavelength is 353 nm, the maximum emission peak of \mathbf{U}_3 is 523 nm, other emission peaks are 501, 546, and 573 nm.

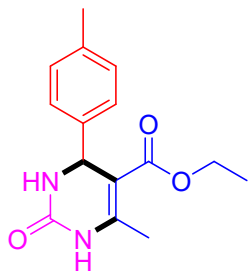
4. Characterization of Products⁹



ethyl 6-methyl-2-oxo-4-phenyl-1,2,3,4-tetrahydropyrimidine-5-carboxylate (4a)

¹H NMR (500 MHz, DMSO-*d*₆): δ (ppm) 9.27 (s, 1H), 7.80 (s, 1H), 7.29 (dd, *J* = 31.2, 11.3 Hz, 5H), 5.18 (s, 1H), 3.98 (d, *J* = 7.3 Hz, 2H), 2.27 (s, 3H), 1.09 (s, 3H);

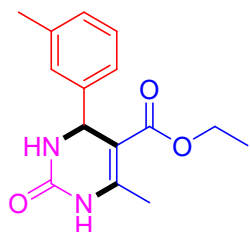
¹³C NMR (126 MHz, DMSO-*d*₆): δ (ppm) 165.80, 152.71, 148.82, 145.33, 128.85, 127.74, 126.73, 99.74, 59.67, 54.46, 18.25, 14.51.



ethyl 6-methyl-2-oxo-4-(p-tolyl)-1,2,3,4-tetrahydropyrimidine-5-carboxylate (4b)

¹H NMR (500 MHz, DMSO-*d*₆): δ (ppm) 9.21 (s, 1H), 7.73 (s, 1H), 7.17 – 7.08 (m, 4H), 5.13 (d, *J* = 3.3 Hz, 1H), 3.98 (q, *J* = 7.1 Hz, 2H), 2.26 (s, 6H), 1.10 (t, *J* = 7.1 Hz, 3H);

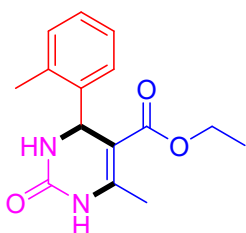
¹³C NMR (126 MHz, DMSO-*d*₆): δ (ppm) 165.83, 152.74, 148.61, 142.42, 136.85, 129.35, 126.63, 99.90, 59.64, 54.12, 21.08, 18.23, 14.53.



ethyl 6-methyl-2-oxo-4-(m-tolyl)-1,2,3,4-tetrahydropyrimidine-5-carboxylate (4c)

¹H NMR (500 MHz, DMSO-*d*₆): δ (ppm) 9.21 (s, 1H), 7.74 (s, 1H), 7.21 (t, *J* = 7.6 Hz, 1H), 7.08 – 7.03 (m, 3H), 5.14 (d, *J* = 3.3 Hz, 1H), 3.99 (qq, *J* = 6.9, 3.8 Hz, 2H), 2.27 (d, *J* = 9.4 Hz, 6H), 1.11 (t, *J* = 7.1 Hz, 3H);

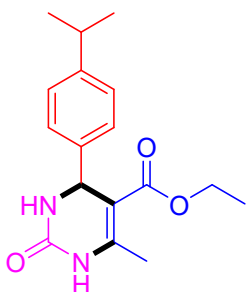
¹³C NMR (126 MHz, DMSO-*d*₆): δ (ppm) 165.82, 152.67, 148.70, 145.34, 137.81, 128.77, 128.36, 127.34, 123.83, 99.76, 59.64, 54.45, 21.59, 18.26, 14.52.



ethyl 6-methyl-2-oxo-4-(*o*-tolyl)-1,2,3,4-tetrahydropyrimidine-5-carboxylate (4d)

¹H NMR (500 MHz, DMSO-*d*₆): δ (ppm) 9.21 (s, 1H), 7.68 (s, 1H), 7.21 – 7.09 (m, 4H), 5.42 (s, 1H), 3.94 – 3.84 (m, 2H), 2.43 (s, 3H), 2.31 (s, 3H), 0.99 (t, *J* = 7.1 Hz, 3H);

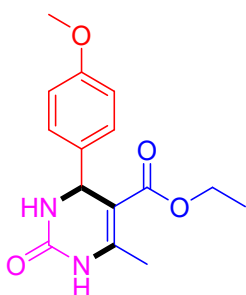
¹³C NMR (126 MHz, DMSO-*d*₆): δ (ppm) 165.71, 152.11, 148.90, 143.72, 135.13, 130.56, 127.63, 127.00, 99.65, 59.54, 50.90, 19.12, 18.14, 14.37.



ethyl 4-(4-isopropylphenyl)-6-methyl-2-oxo-1,2,3,4-tetrahydropyrimidine-5-carboxylate (4e)

¹H NMR (500 MHz, DMSO-*d*₆): δ (ppm) 9.22 (s, 1H), 7.73 (s, 1H), 7.18 (s, 4H), 5.14 (d, *J* = 3.4 Hz, 1H), 3.99 (q, *J* = 7.1 Hz, 2H), 2.84 (hept, *J* = 7.0 Hz, 1H), 2.26 (s, 3H), 1.17 (d, *J* = 7.0 Hz, 6H), 1.11 (t, *J* = 7.1 Hz, 3H);

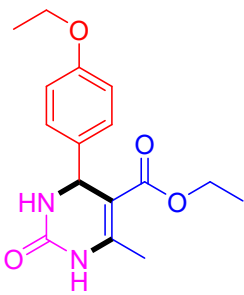
¹³C NMR (126 MHz, DMSO-*d*₆): δ (ppm) 165.86, 152.80, 148.62, 147.86, 142.85, 126.71, 126.66, 99.94, 59.66, 54.10, 33.60, 24.35, 24.30, 18.26, 14.53.



ethyl 4-(4-methoxyphenyl)-6-methyl-2-oxo-1,2,3,4-tetrahydropyrimidine-5-carboxylate (4f)

¹H NMR (500 MHz, DMSO-*d*₆): δ (ppm) 9.20 (s, 1H), 7.71 (s, 1H), 7.16 (d, *J* = 8.5 Hz, 2H), 6.88 (d, *J* = 8.6 Hz, 2H), 5.12 (d, *J* = 3.3 Hz, 1H), 3.98 (q, *J* = 7.1 Hz, 2H), 3.72 (s, 3H), 2.26 (s, 3H), 1.10 (t, *J* = 7.1 Hz, 3H);

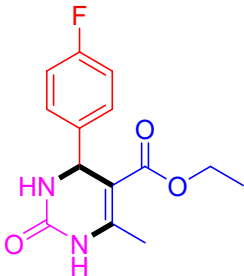
¹³C NMR (126 MHz, DMSO-*d*₆): δ (ppm) 165.84, 158.91, 152.69, 148.47, 137.52, 127.88, 114.15, 100.05, 59.63, 55.48, 53.82, 18.22, 14.54.



ethyl 4-(4-ethoxyphenyl)-6-methyl-2-oxo-1,2,3,4-tetrahydropyrimidine-5-carboxylate (4g)

¹H NMR (500 MHz, DMSO-*d*₆): δ (ppm) 9.19 (s, 1H), 7.70 (s, 1H), 7.14 (d, *J* = 8.3 Hz, 2H), 6.86 (d, *J* = 8.3 Hz, 2H), 5.10 (d, *J* = 3.2 Hz, 1H), 3.97 (dd, *J* = 7.1, 3.2 Hz, 4H), 2.25 (s, 3H), 1.29 (t, *J* = 7.0 Hz, 3H), 1.09 (t, *J* = 7.1 Hz, 3H);

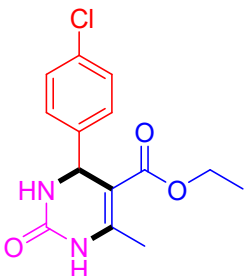
¹³C NMR (126 MHz, DMSO-*d*₆): δ (ppm) 165.85, 158.19, 152.70, 148.45, 137.38, 127.88, 114.60, 100.05, 63.40, 59.62, 53.83, 18.22, 15.08, 14.54.



ethyl 4-(4-fluorophenyl)-6-methyl-2-oxo-1,2,3,4-tetrahydropyrimidine-5-carboxylate (4h)

¹H NMR (500 MHz, DMSO-*d*₆): δ (ppm) 9.27 (s, 1H), 7.79 (s, 1H), 7.28 (t, *J* = 6.1 Hz, 2H), 7.14 (t, *J* = 7.7 Hz, 2H), 5.17 (s, 1H), 3.98 (dtd, *J* = 9.4, 7.1, 3.7 Hz, 2H), 2.26 (s, 3H), 1.08 (td, *J* = 7.1, 2.2 Hz, 3H);

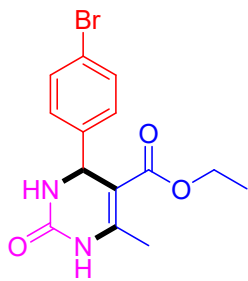
¹³C NMR (126 MHz, DMSO-*d*₆): δ (ppm) 165.71, 152.53, 148.98, 141.60, 128.73 (d, *J* = 8.2 Hz), 115.65, 115.48, 99.61, 59.68, 53.84, 18.24, 14.47.



ethyl 4-(4-chlorophenyl)-6-methyl-2-oxo-1,2,3,4-tetrahydropyrimidine-5-carboxylate (4i)

¹H NMR (500 MHz, DMSO-*d*₆): δ (ppm) 9.28 (s, 1H), 7.81 (s, 1H), 7.53 (d, *J* = 8.0 Hz, 2H), 7.20 (d, *J* = 8.0 Hz, 2H), 5.14 (s, 1H), 3.98 (q, *J* = 7.1 Hz, 2H), 2.26 (s, 3H), 1.09 (t, *J* = 7.1 Hz, 3H);

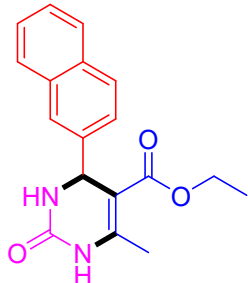
¹³C NMR (126 MHz, DMSO-*d*₆): δ (ppm) 165.66, 152.45, 149.20, 144.66, 131.79, 129.03, 120.80, 99.24, 59.75, 53.97, 18.29, 14.53.



ethyl 4-(4-bromophenyl)-6-methyl-2-oxo-1,2,3,4-tetrahydropyrimidine-5-carboxylate (4j)

¹H NMR (500 MHz, DMSO-*d*₆): δ (ppm) 9.30 (s, 1H), 7.82 (s, 1H), 7.39 (d, *J* = 8.4 Hz, 2H), 7.27 (d, *J* = 8.6 Hz, 2H), 5.18 (d, *J* = 3.4 Hz, 1H), 3.98 (qd, *J* = 7.1, 2.1 Hz, 2H), 2.27 (s, 3H), 1.09 (t, *J* = 7.1 Hz, 3H);

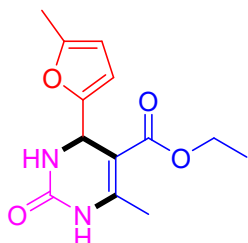
¹³C NMR (126 MHz, DMSO-*d*₆): δ (ppm) 165.67, 152.51, 149.16, 144.25, 132.30, 128.84, 128.66, 99.33, 59.73, 53.94, 18.27, 14.49.



ethyl 6-methyl-4-(naphthalen-2-yl)-2-oxo-1,2,3,4-tetrahydropyrimidine-5-carboxylate (4k)

¹H NMR (500 MHz, DMSO-*d*₆): δ (ppm) 9.34 (s, 1H), 7.89 (dt, *J* = 11.7, 6.6 Hz, 4H), 7.72 (s, 1H), 7.53 – 7.45 (m, 3H), 5.39 (d, *J* = 3.3 Hz, 1H), 3.98 (q, *J* = 7.1 Hz, 2H), 2.34 (s, 3H), 1.08 (t, *J* = 7.1 Hz, 3H);

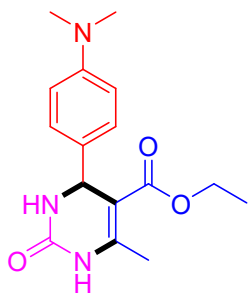
¹³C NMR (126 MHz, DMSO-*d*₆): δ (ppm) 165.84, 152.64, 149.05, 142.66, 133.18, 132.83, 128.81, 128.30, 127.94, 126.74, 126.36, 125.40, 125.09, 99.56, 59.69, 54.84, 18.37, 14.53.



ethyl 6-methyl-4-(5-methylfuran-2-yl)-2-oxo-1,2,3,4-tetrahydropyrimidine-5-carboxylate (4l)

¹H NMR (500 MHz, DMSO-*d*₆): δ (ppm) 9.23 (s, 1H), 7.75 (s, 1H), 5.94 (s, 2H), 5.16 (d, *J* = 3.6 Hz, 1H), 4.10 – 3.97 (m, 2H), 2.22 (d, *J* = 17.1 Hz, 6H), 1.14 (t, *J* = 7.1 Hz, 3H);

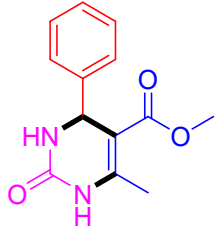
¹³C NMR (126 MHz, DMSO-*d*₆): δ (ppm) 165.52, 154.66, 152.92, 151.18, 149.69, 106.79, 106.48, 97.28, 59.66, 48.18, 18.19, 14.58, 13.82.



ethyl 4-(4-(dimethylamino)phenyl)-6-methyl-2-oxo-1,2,3,4-tetrahydropyrimidine-5-carboxylate (4m)

¹H NMR (500 MHz, DMSO-*d*₆): δ (ppm) 9.05 (s, 1H), 7.55 (s, 1H), 6.97 (d, *J* = 8.4 Hz, 2H), 6.58 (d, *J* = 8.5 Hz, 2H), 4.97 (d, *J* = 3.3 Hz, 1H), 3.90 (qq, *J* = 6.4, 3.8 Hz, 2H), 2.76 (s, 6H), 2.16 (s, 3H), 1.04 (t, *J* = 7.1 Hz, 3H);

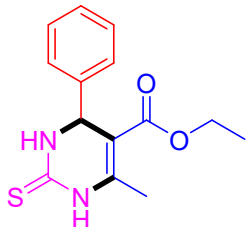
¹³C NMR (126 MHz, DMSO-*d*₆): δ (ppm) 165.96, 152.84, 150.21, 148.02, 133.11, 127.37, 112.67, 100.38, 59.57, 53.79, 18.20, 14.59.



methyl 6-methyl-2-oxo-4-phenyl-1,2,3,4-tetrahydropyrimidine-5-carboxylate (4n)

¹H NMR (500 MHz, DMSO-*d*₆): δ (ppm) 9.28 (s, 1H), 7.81 (s, 1H), 7.36 – 7.22 (m, 5H), 5.18 (s, 1H), 3.54 (s, 3H), 2.28 (s, 3H);

¹³C NMR (126 MHz, DMSO-*d*₆): δ (ppm) 166.32, 152.73, 149.14, 145.14, 128.93, 127.77, 126.66, 99.49, 54.30, 51.25, 18.31.

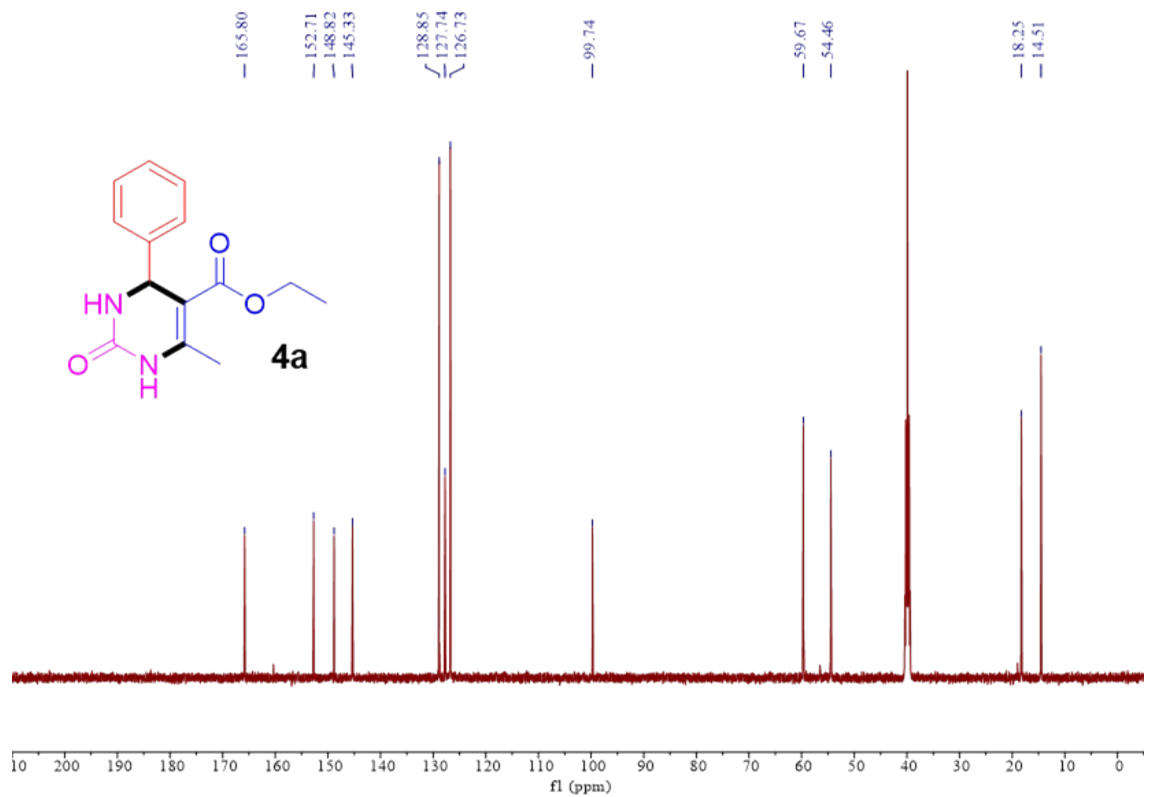
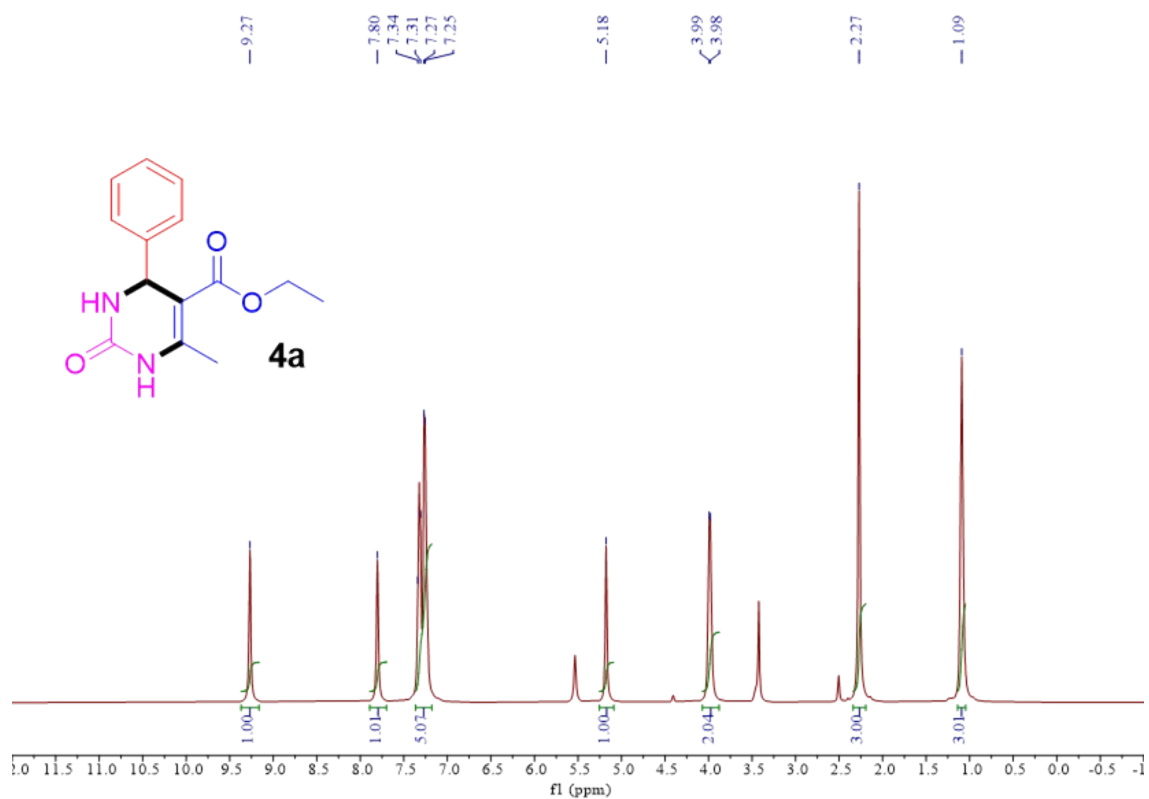


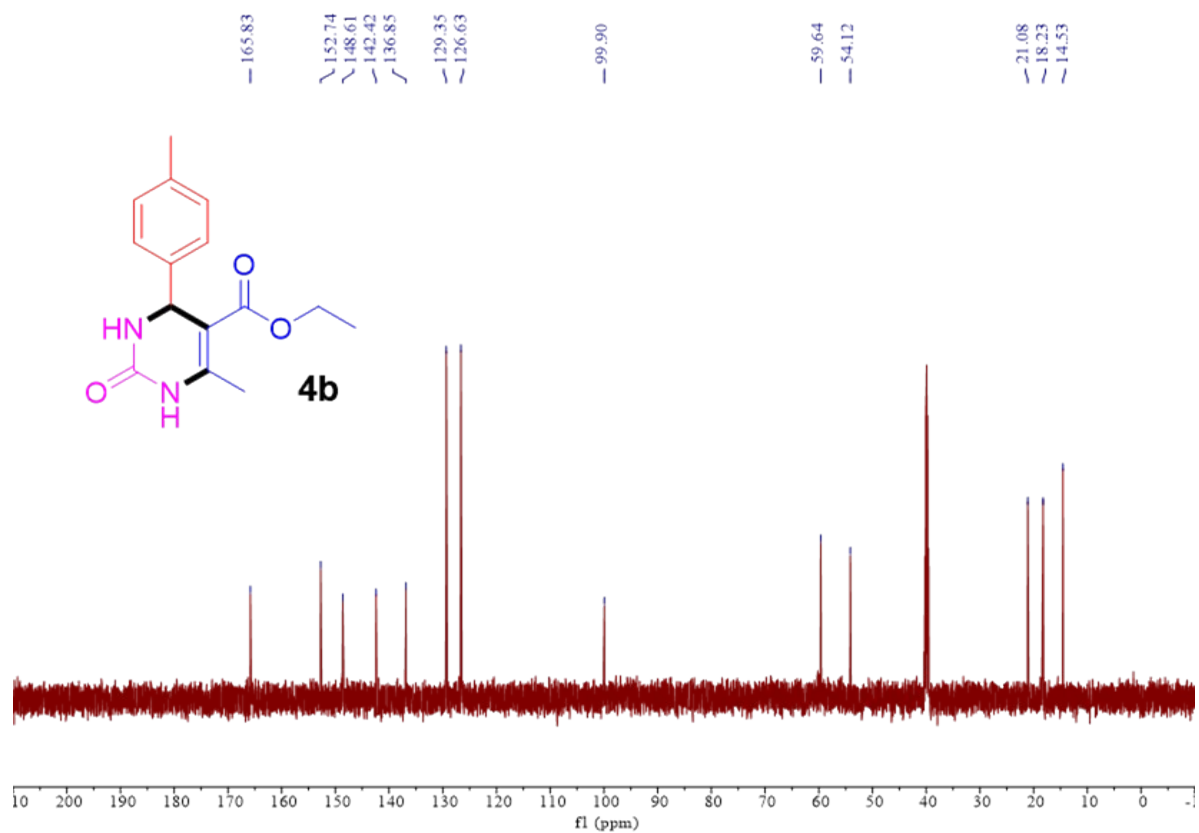
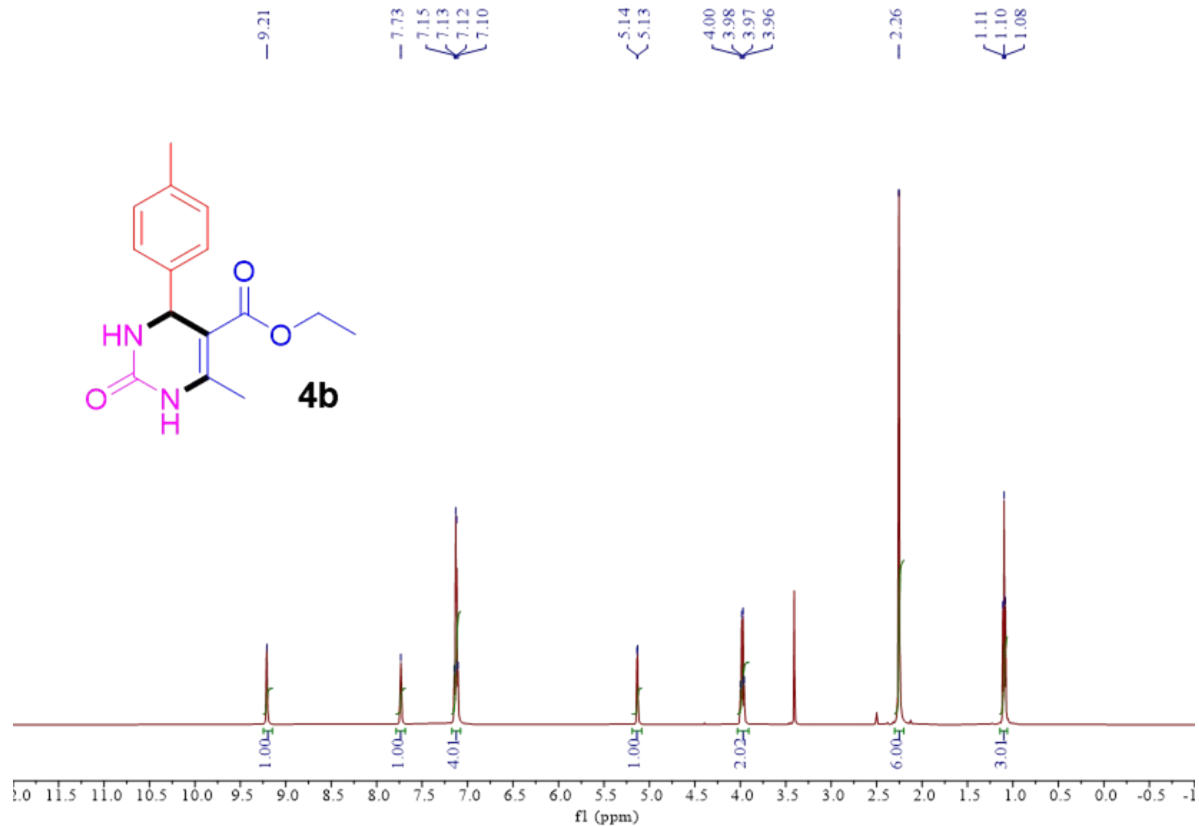
ethyl 6-methyl-4-phenyl-2-thioxo-1,2,3,4-tetrahydropyrimidine-5-carboxylate (4o)

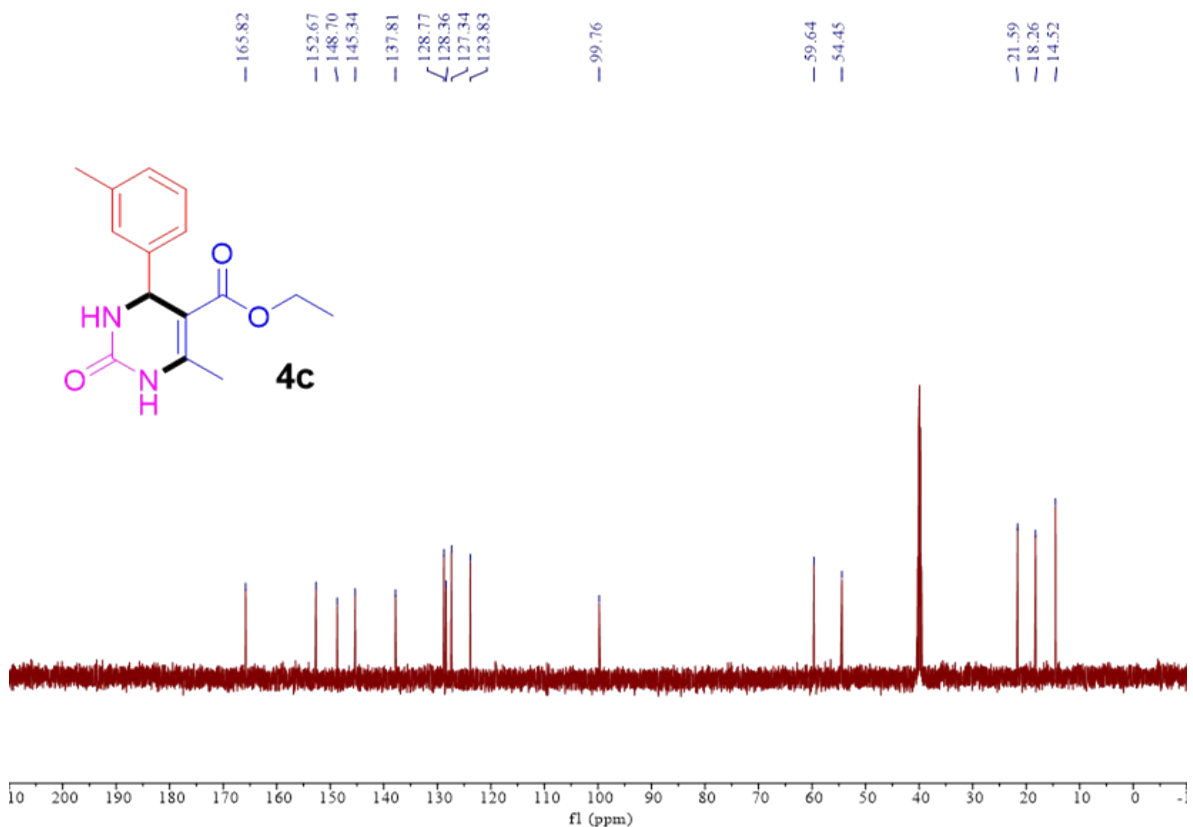
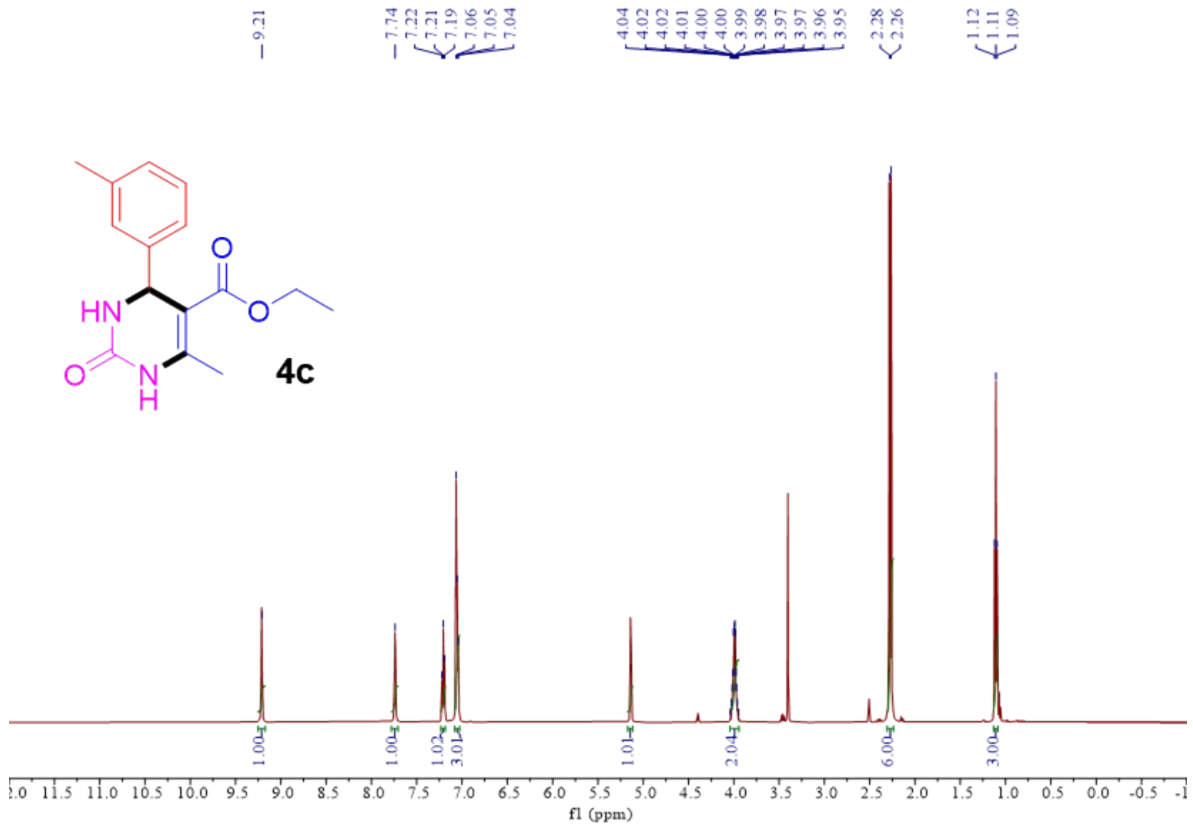
¹H NMR (500 MHz, DMSO-*d*₆): δ (ppm) 10.36 (s, 1H), 9.67 (s, 1H), 7.36 – 7.22 (m, 5H), 5.19 (d, *J* = 3.8 Hz, 1H), 4.00 (q, *J* = 6.9 Hz, 2H), 2.30 (s, 3H), 1.09 (t, *J* = 7.1 Hz, 3H);

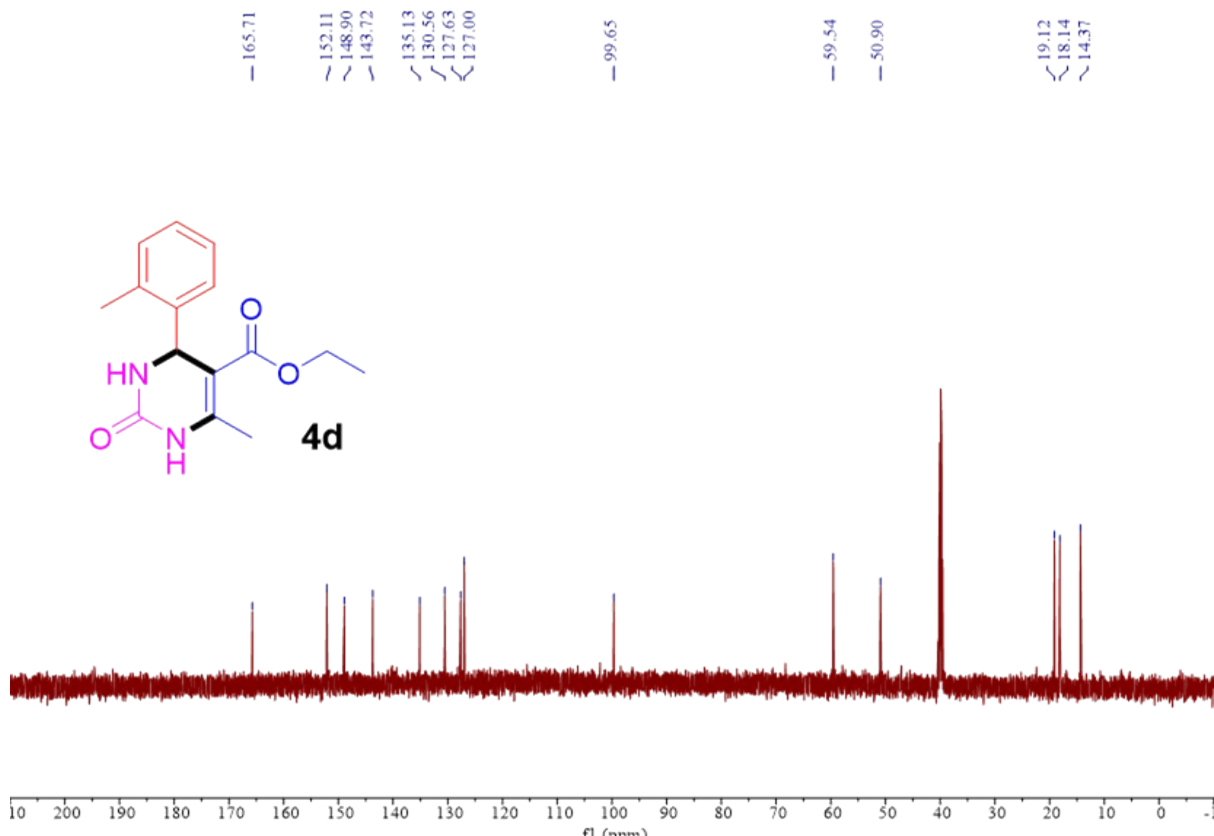
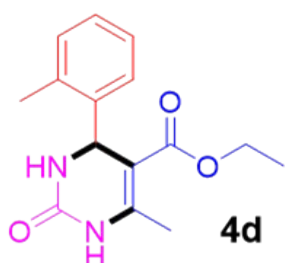
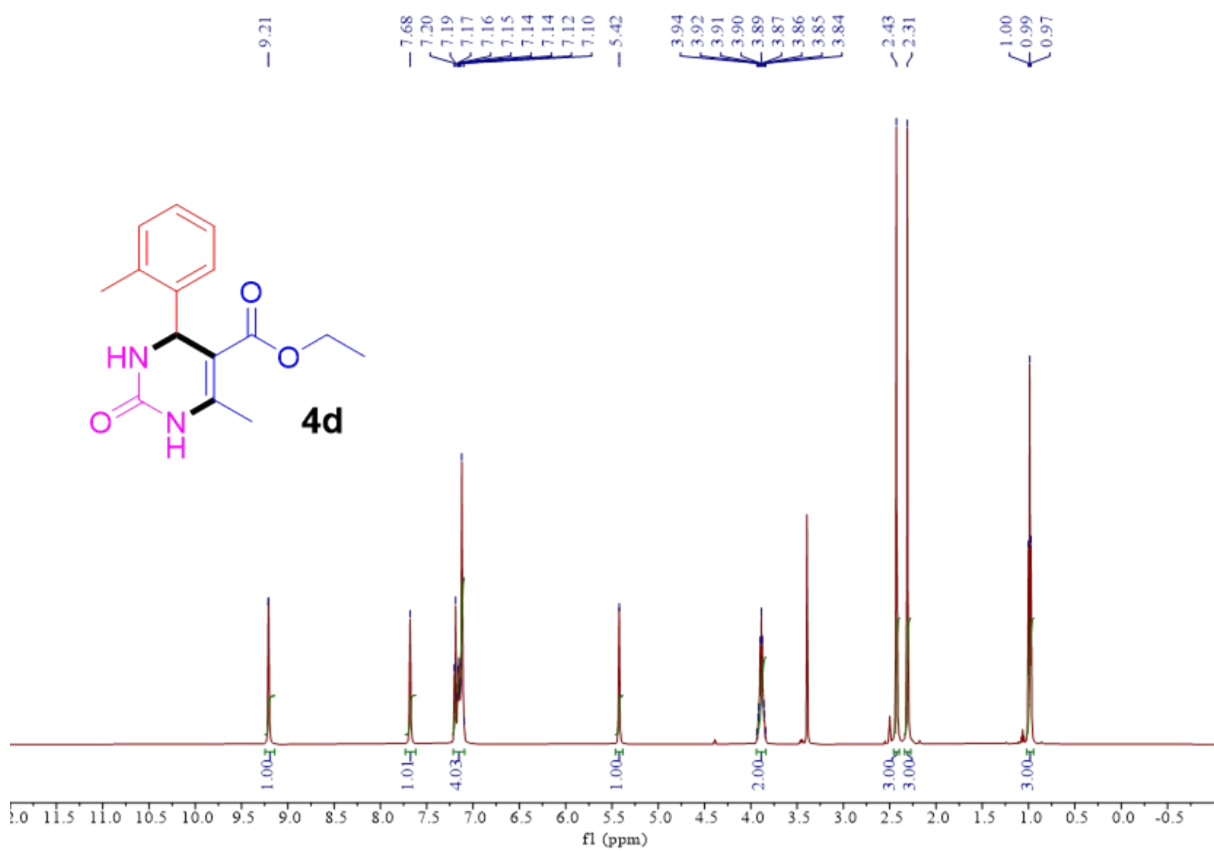
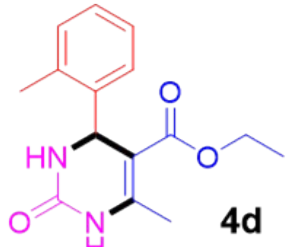
¹³C NMR (126 MHz, DMSO-*d*₆): δ (ppm) 174.70, 165.59, 145.51, 143.97, 129.03, 128.15, 126.87, 101.17, 60.07, 54.52, 17.64, 14.46.

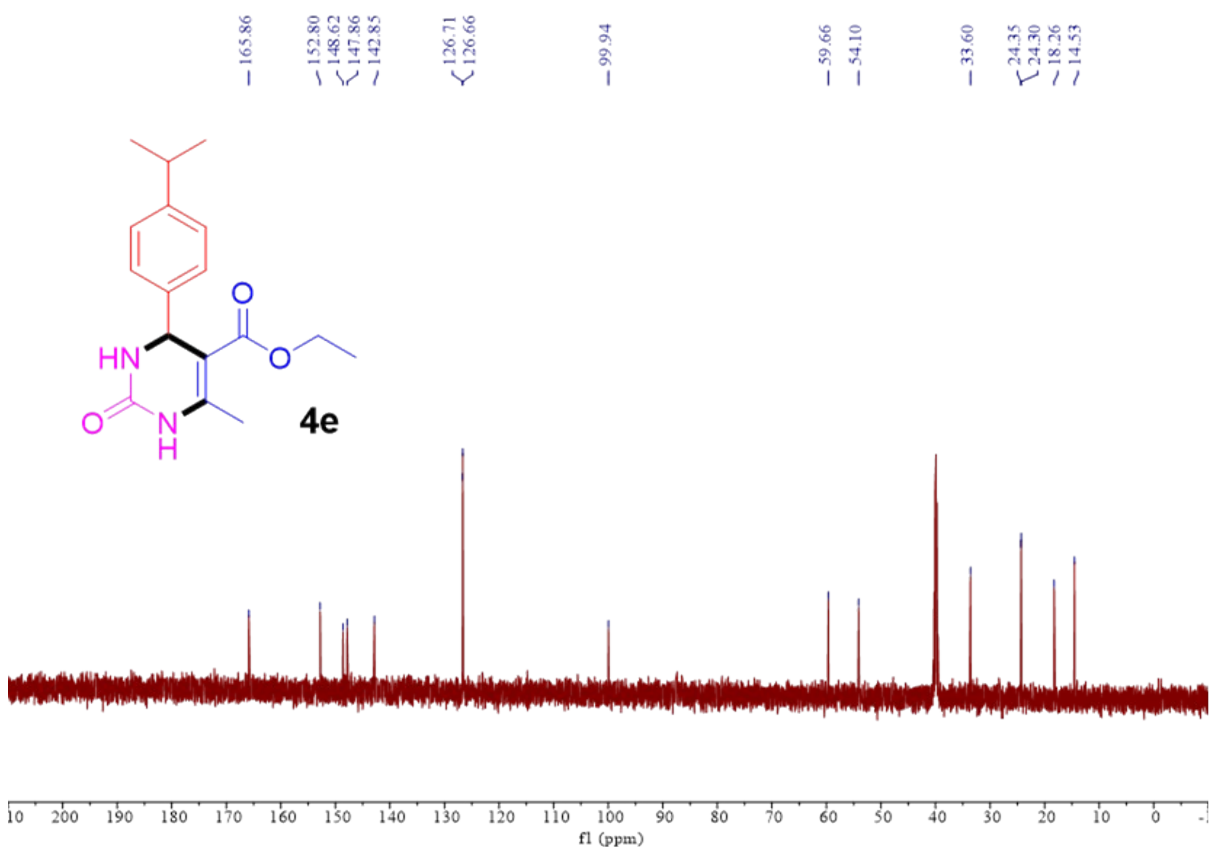
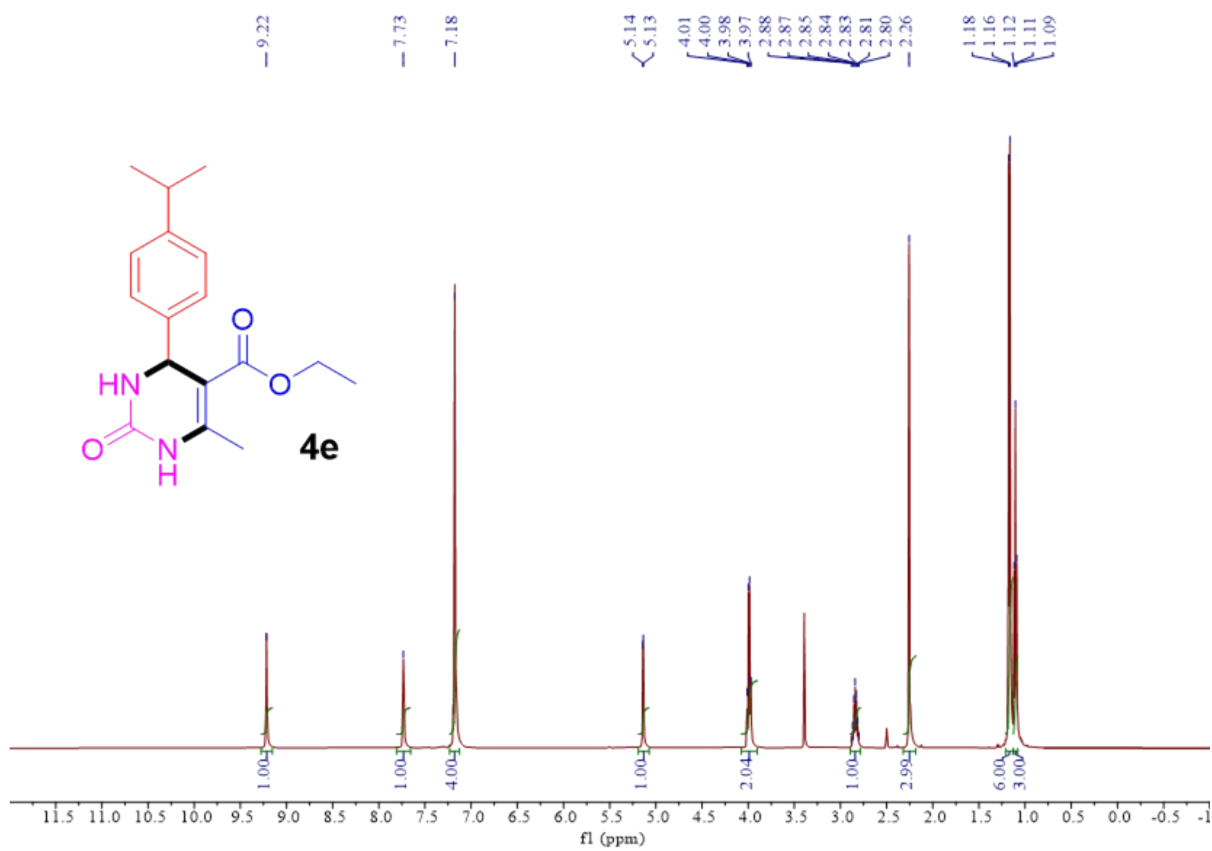
5. NMR Spectra

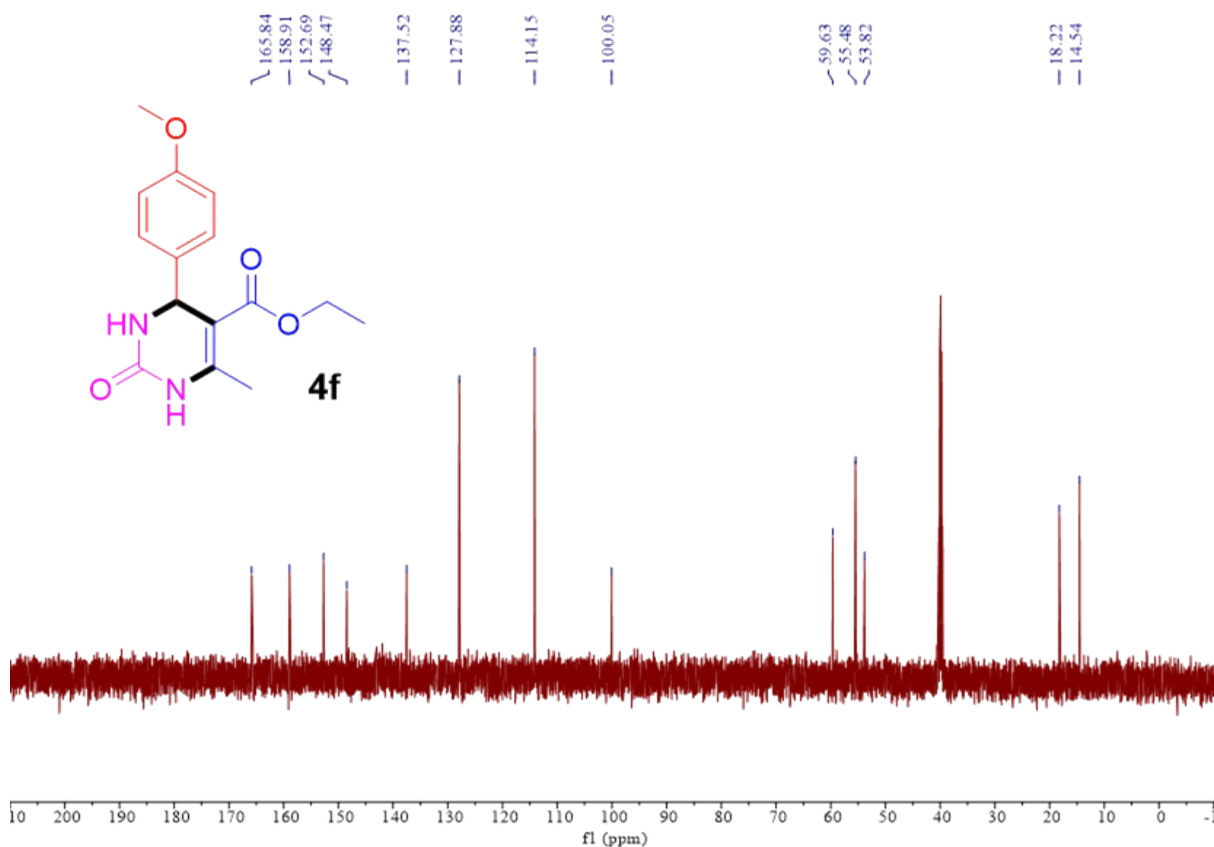
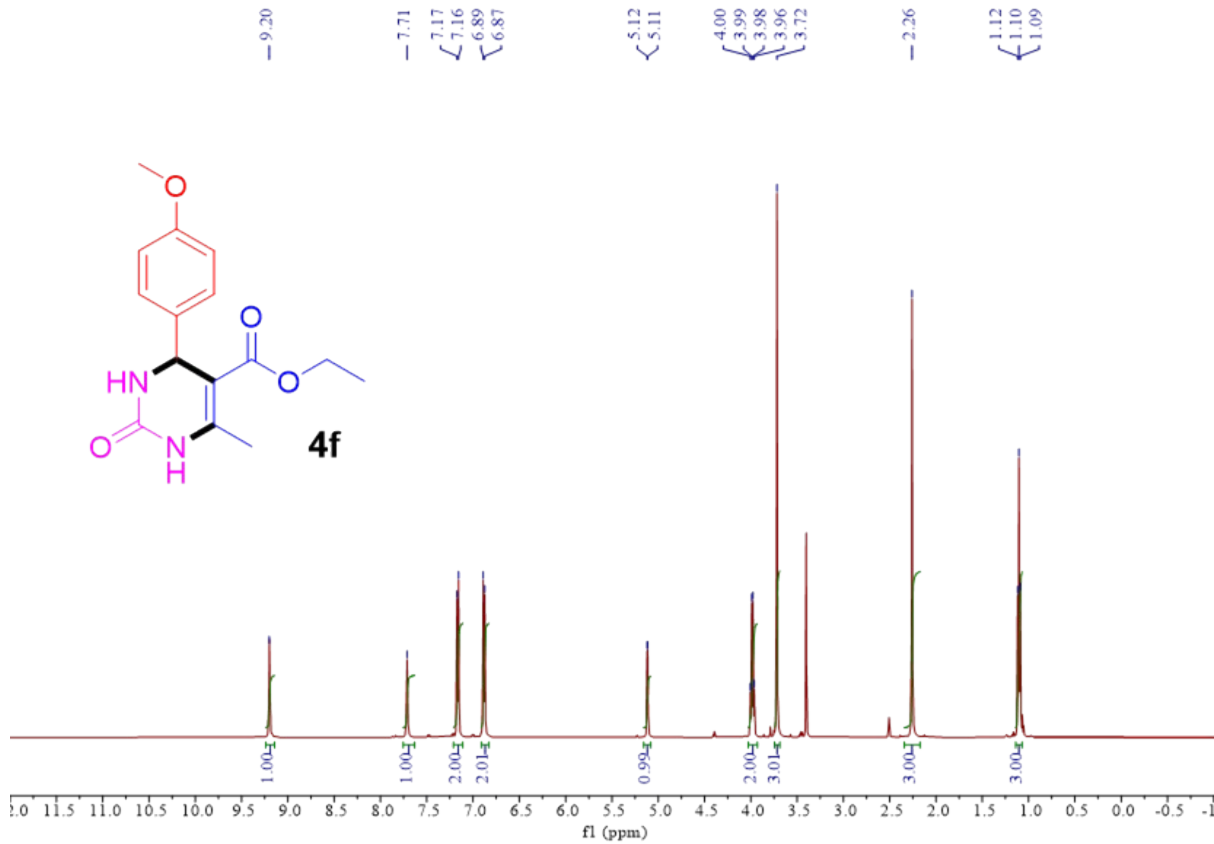


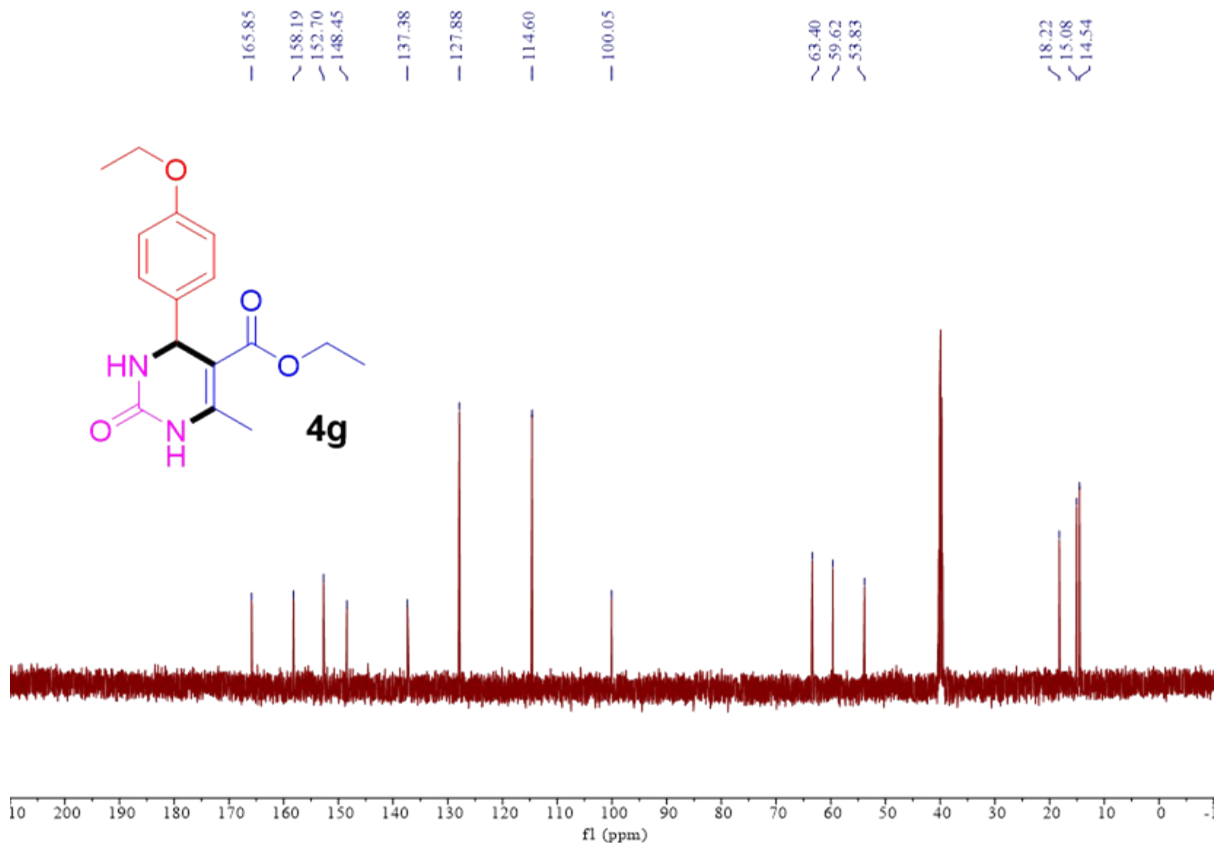
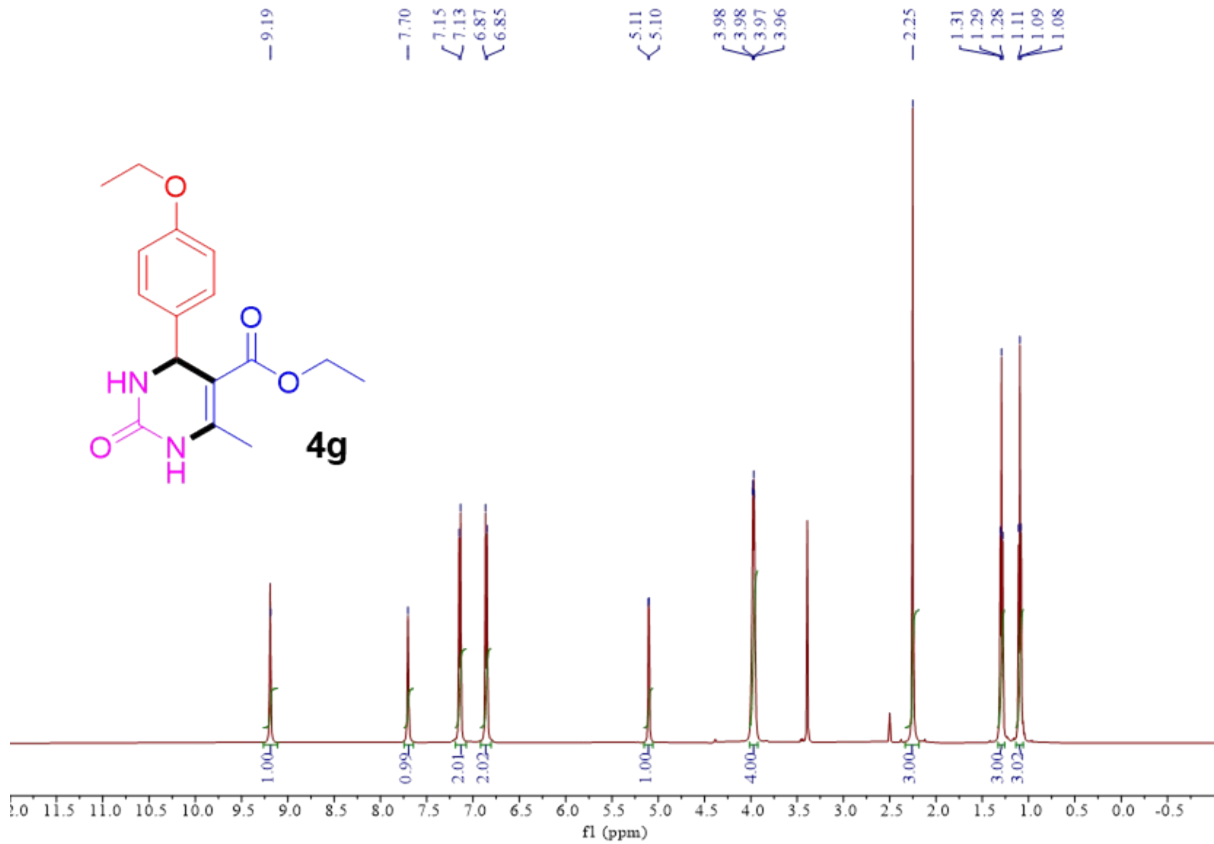


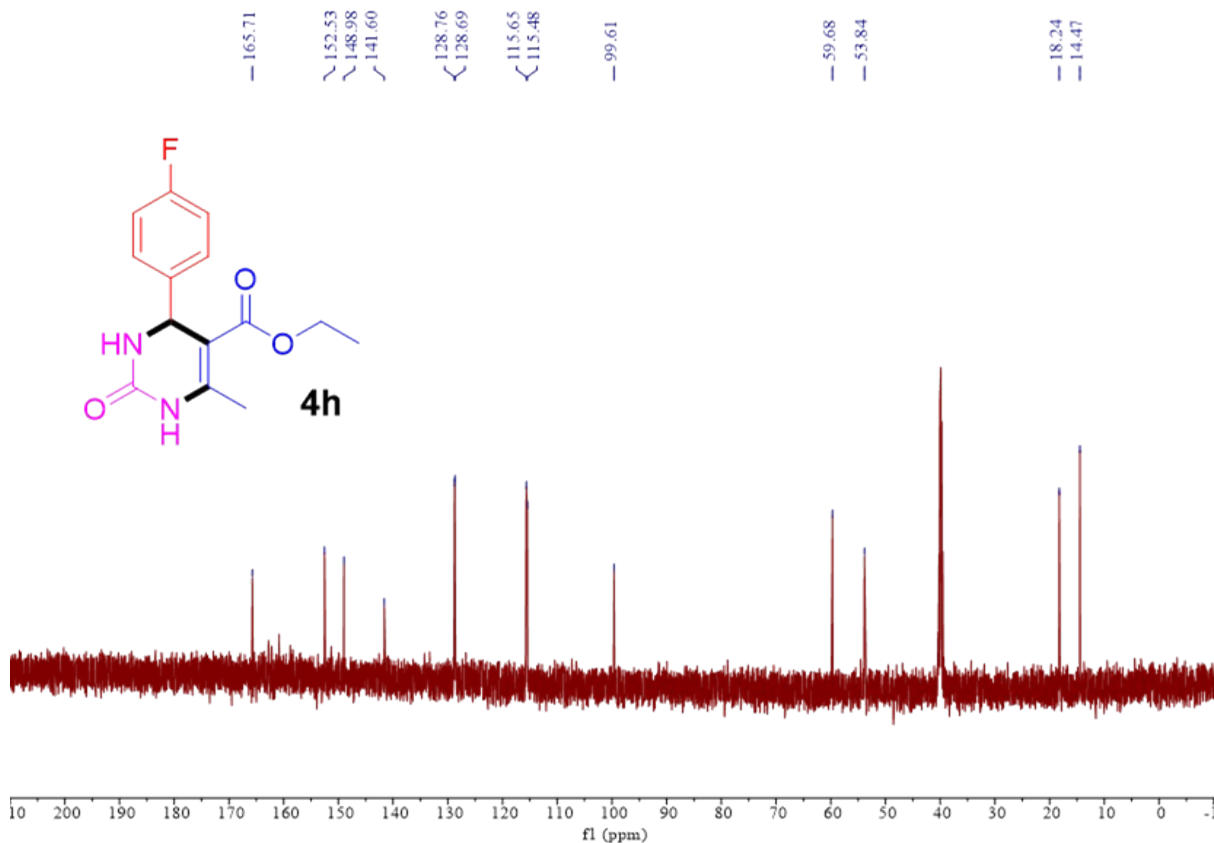
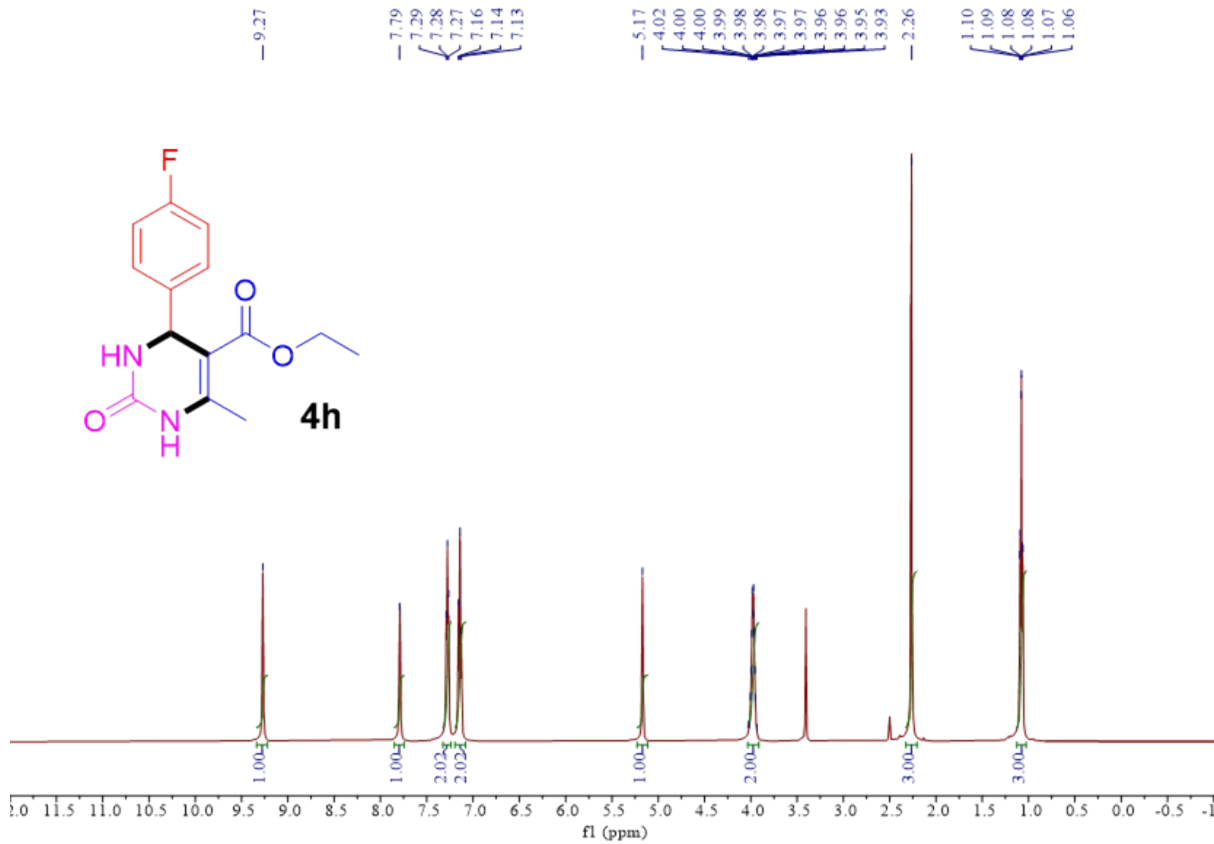


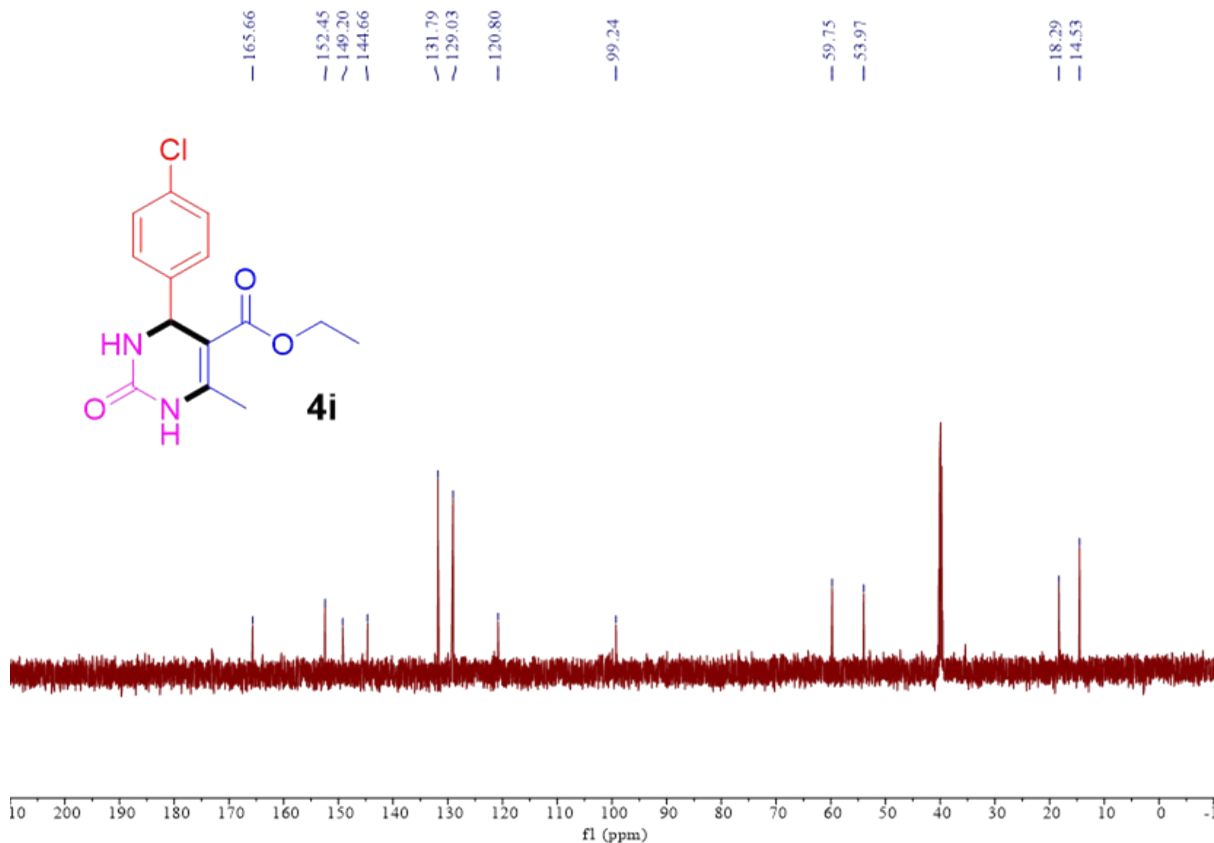
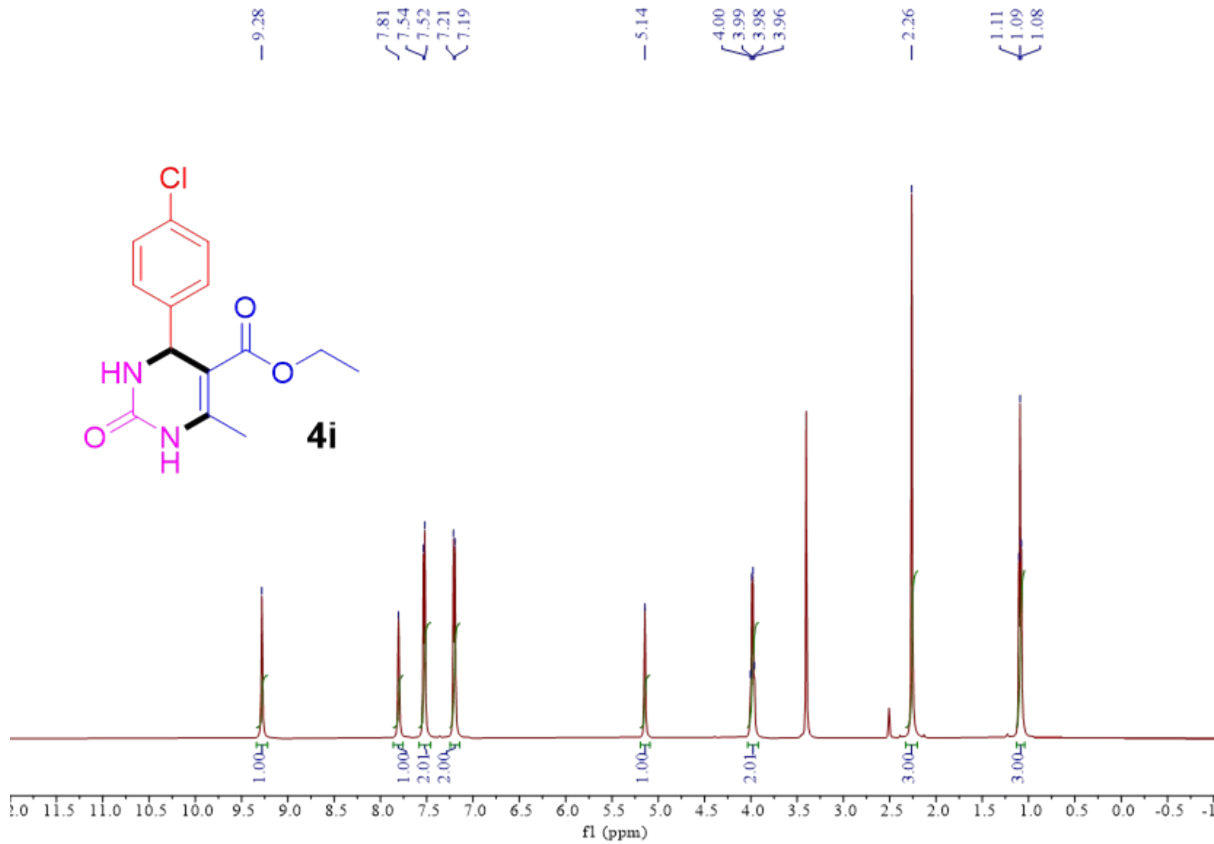


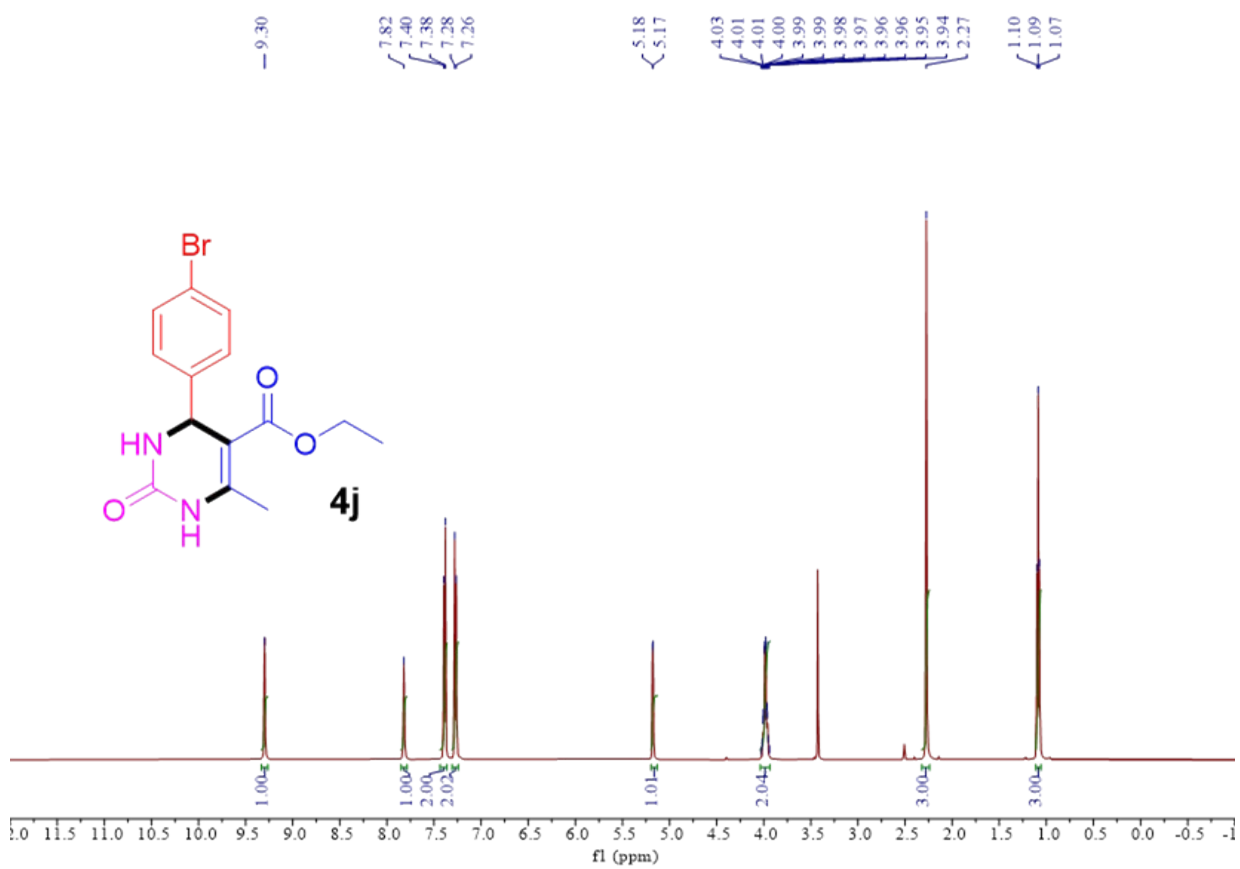
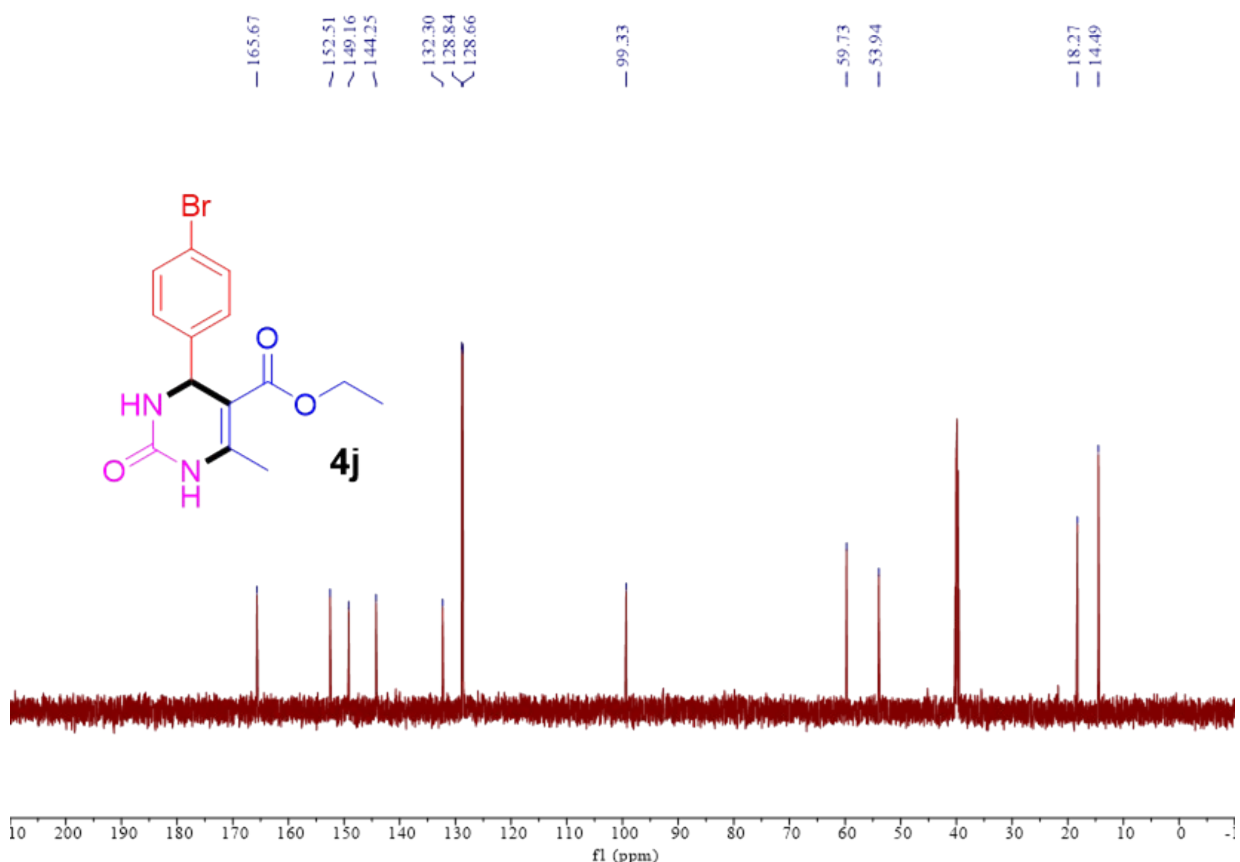


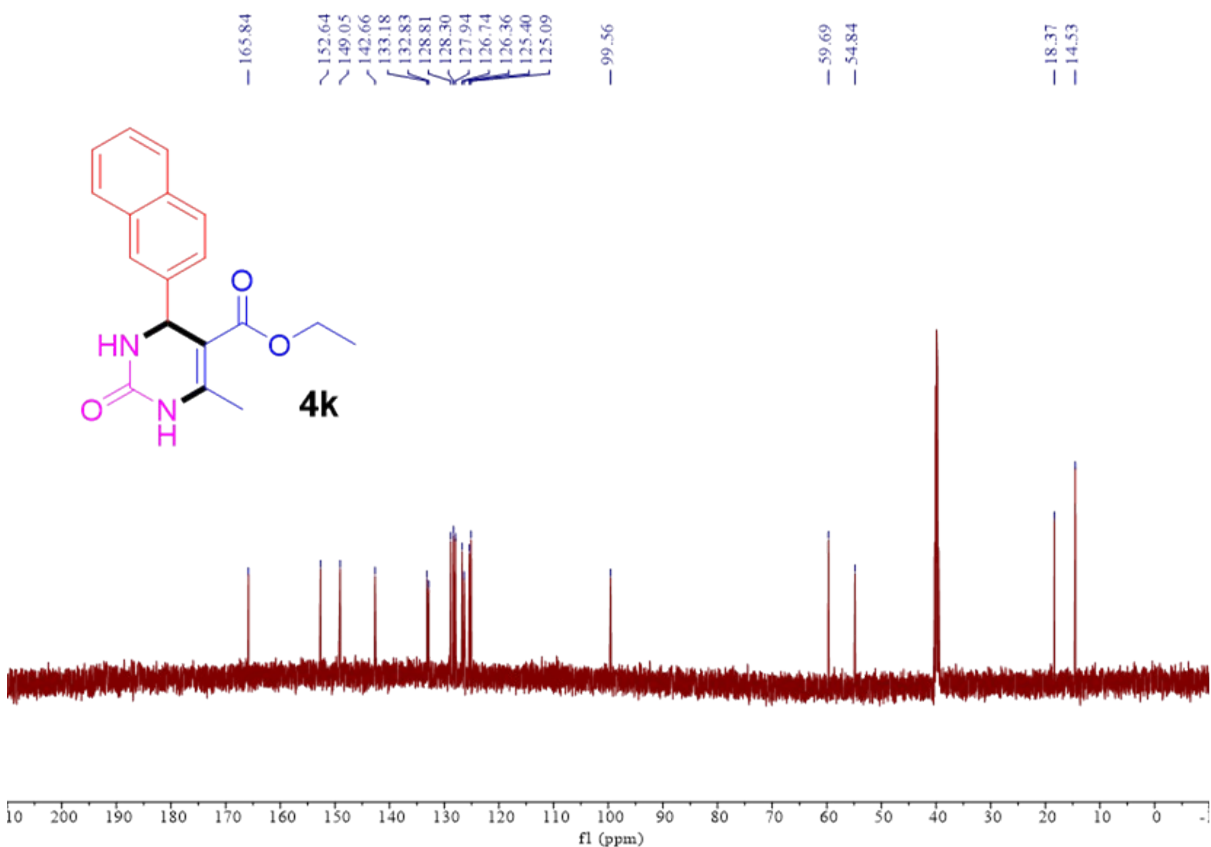
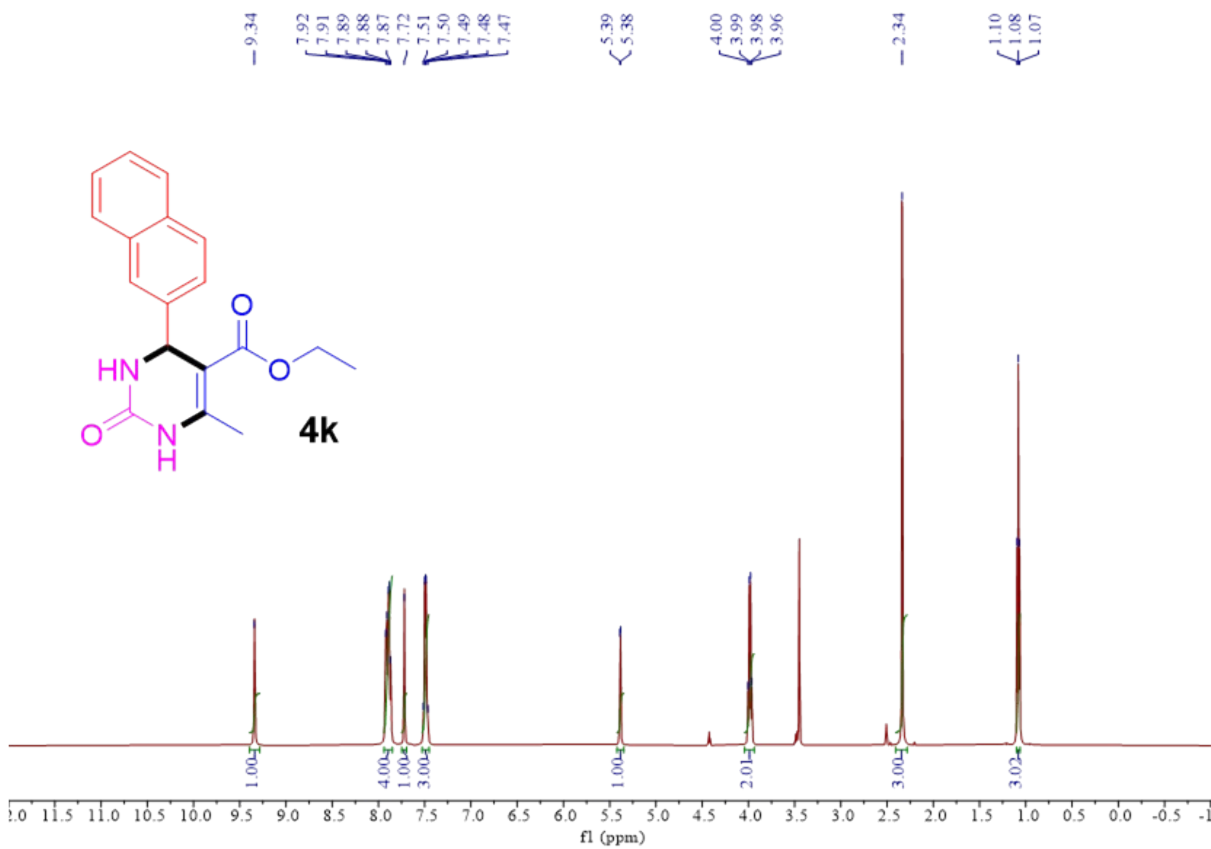


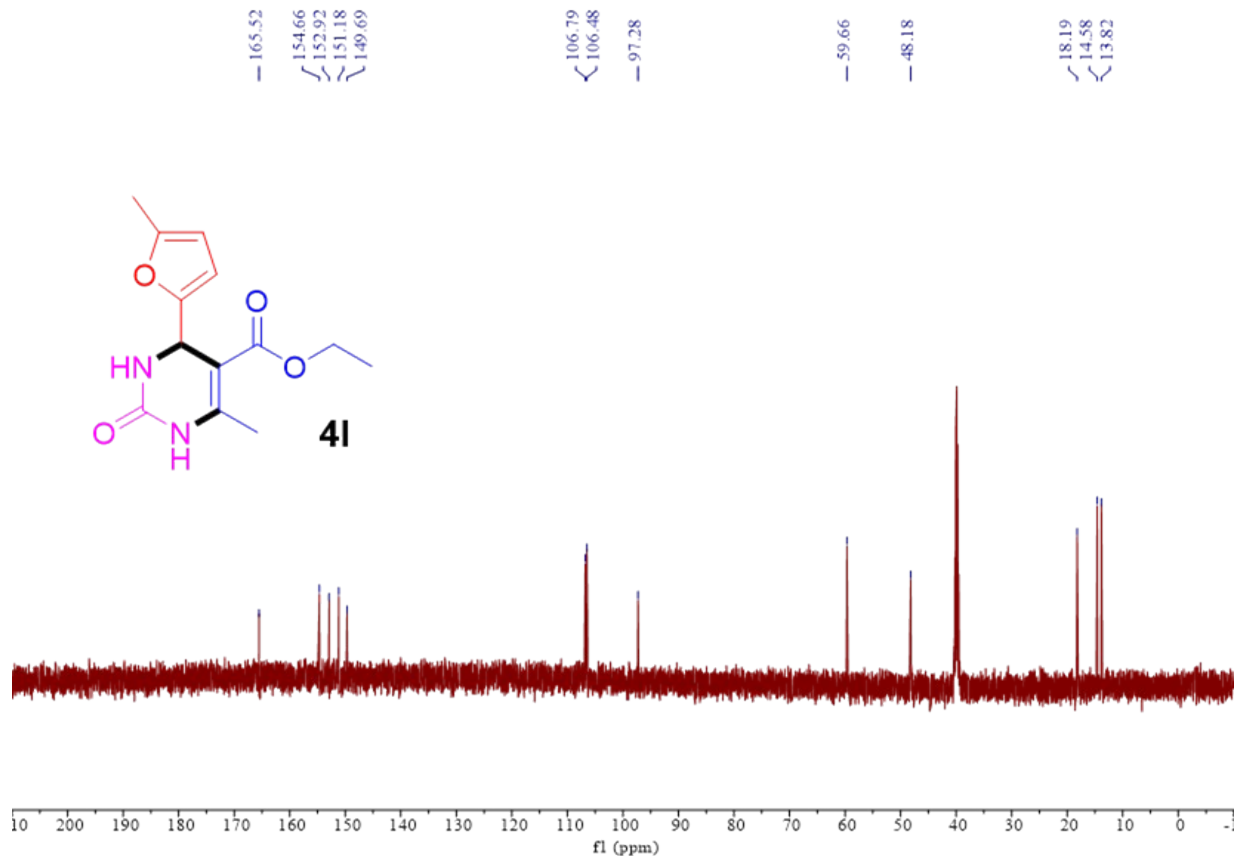
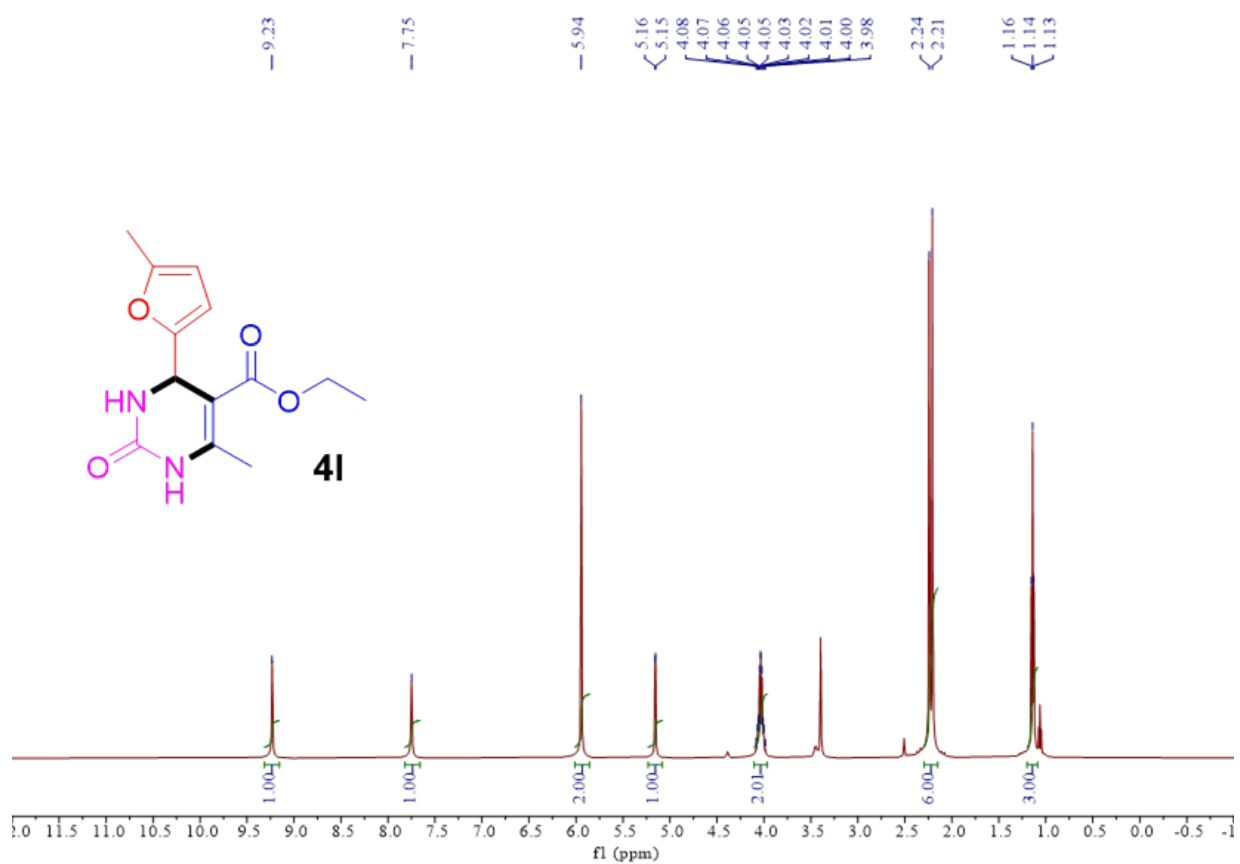


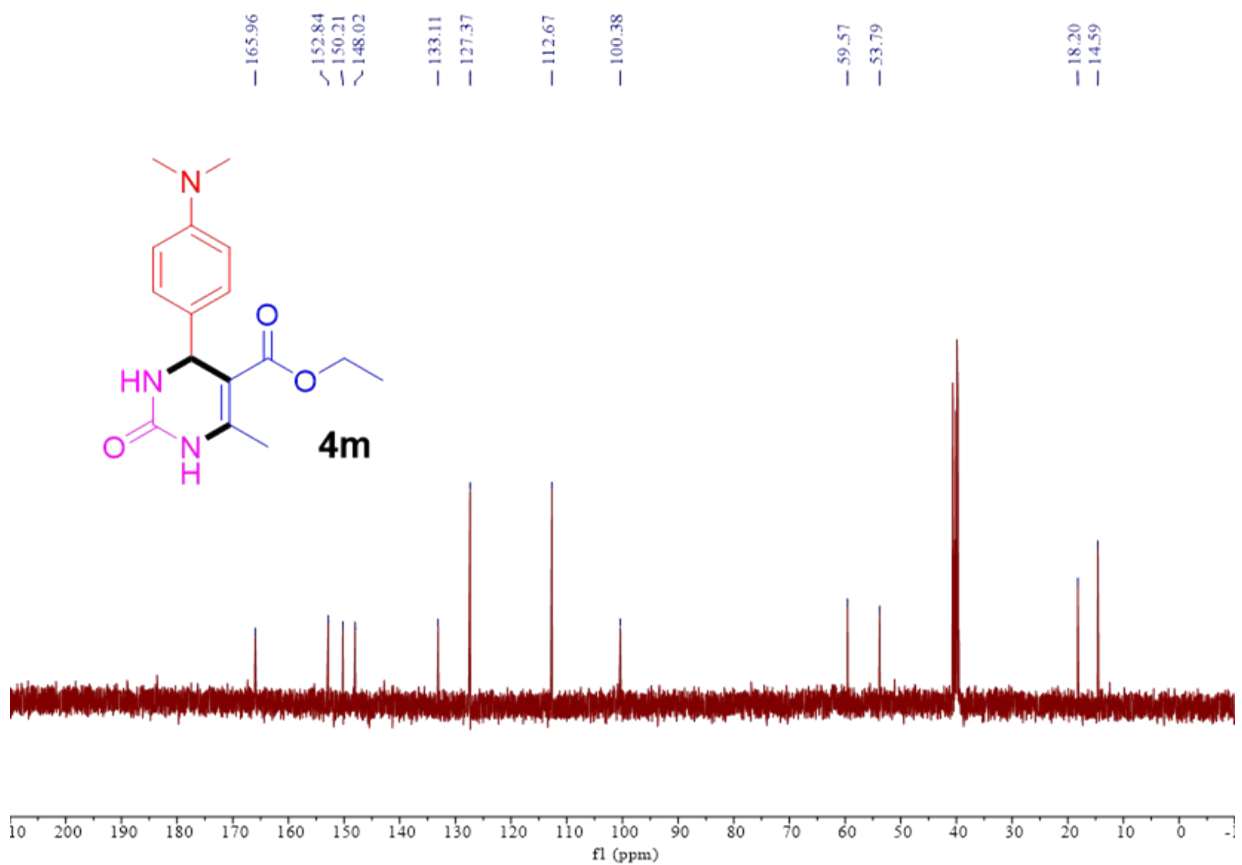
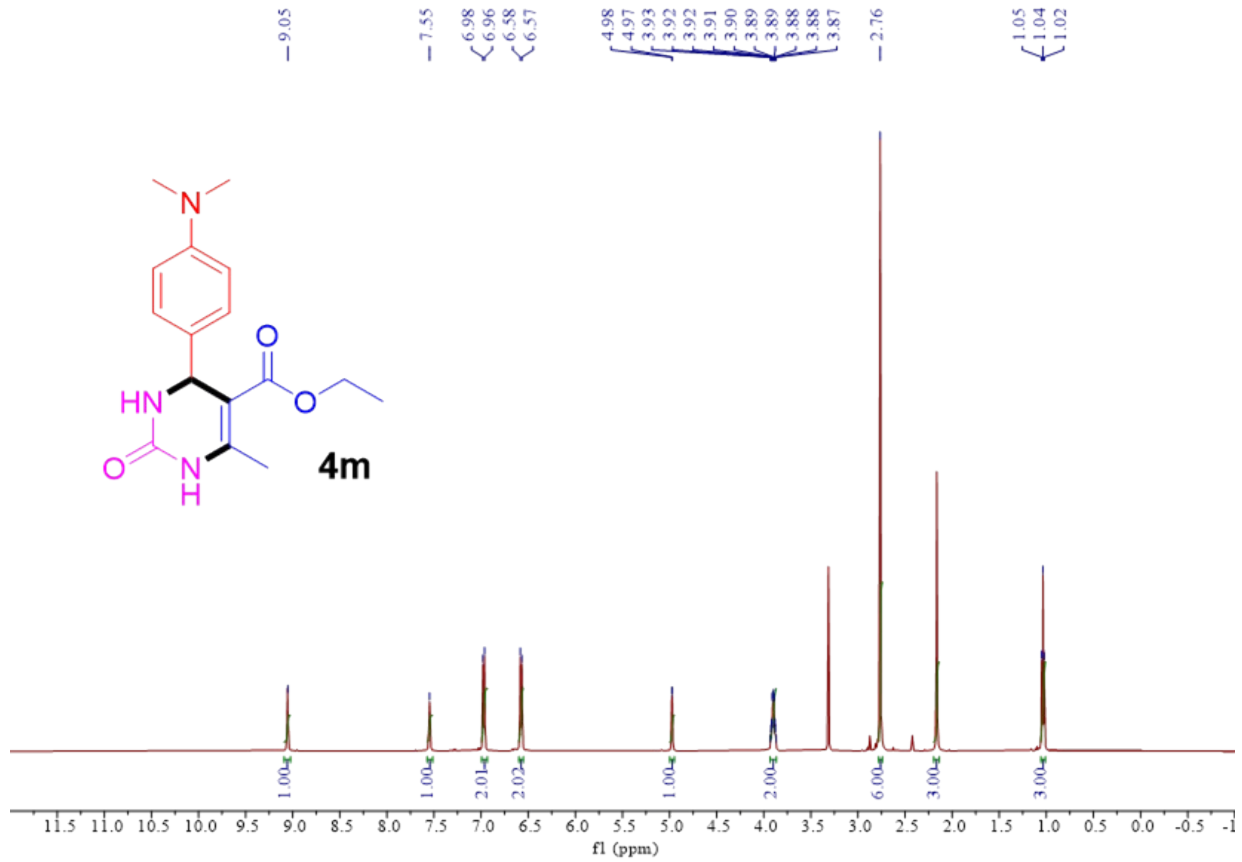


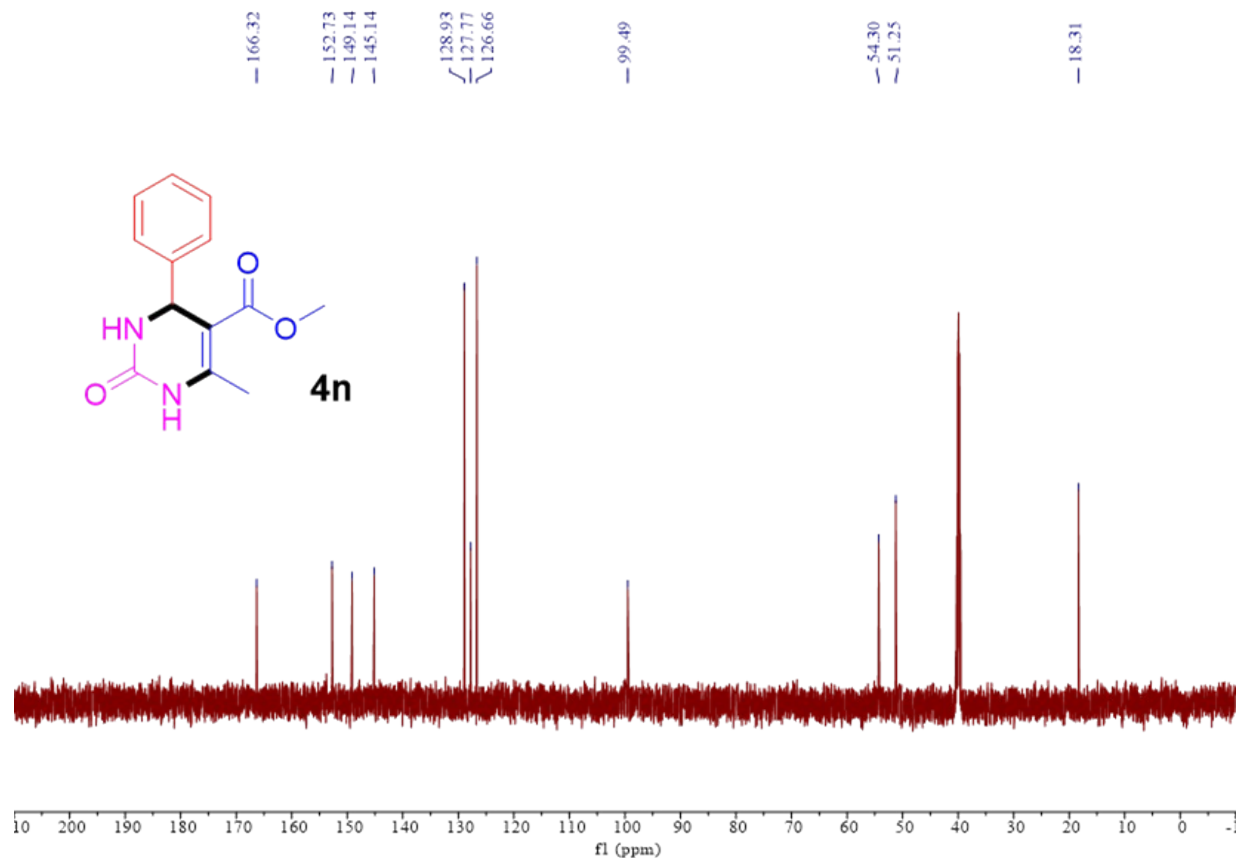
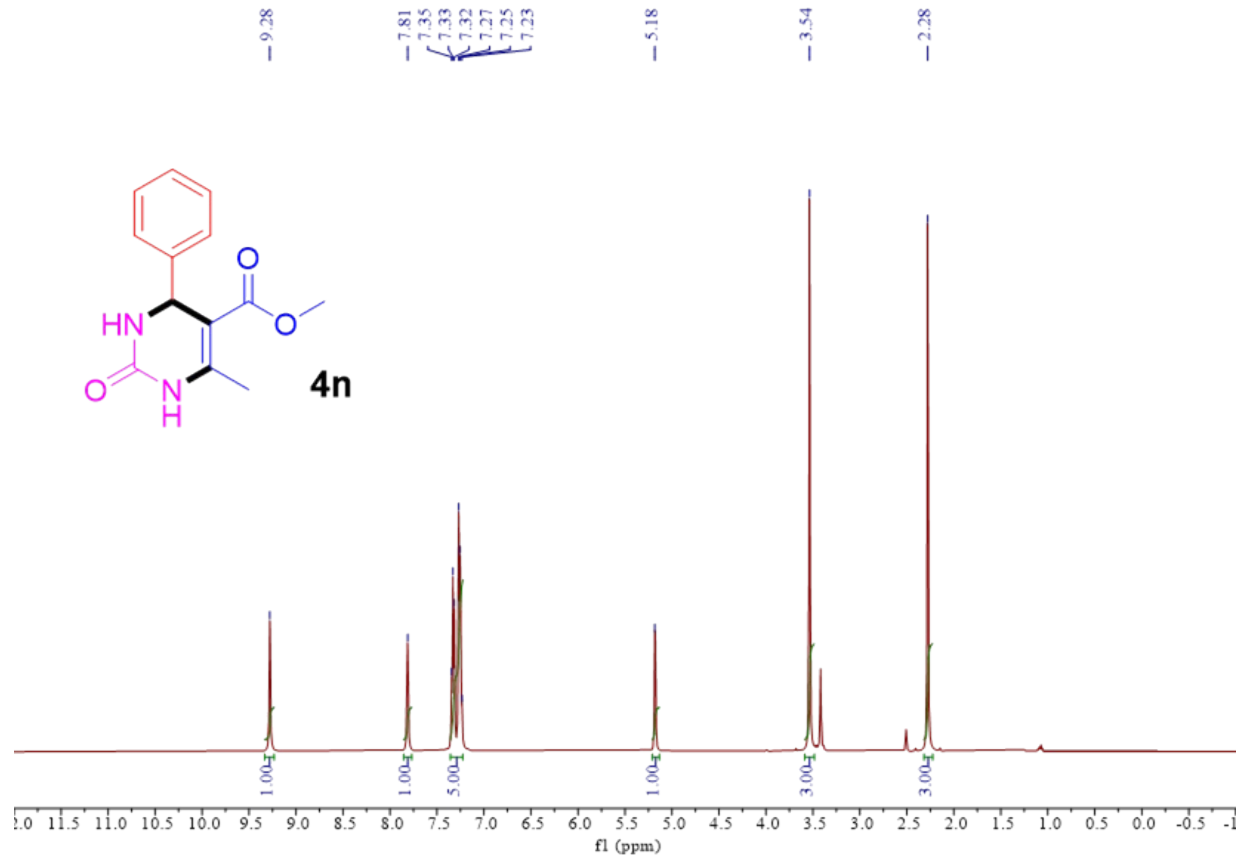


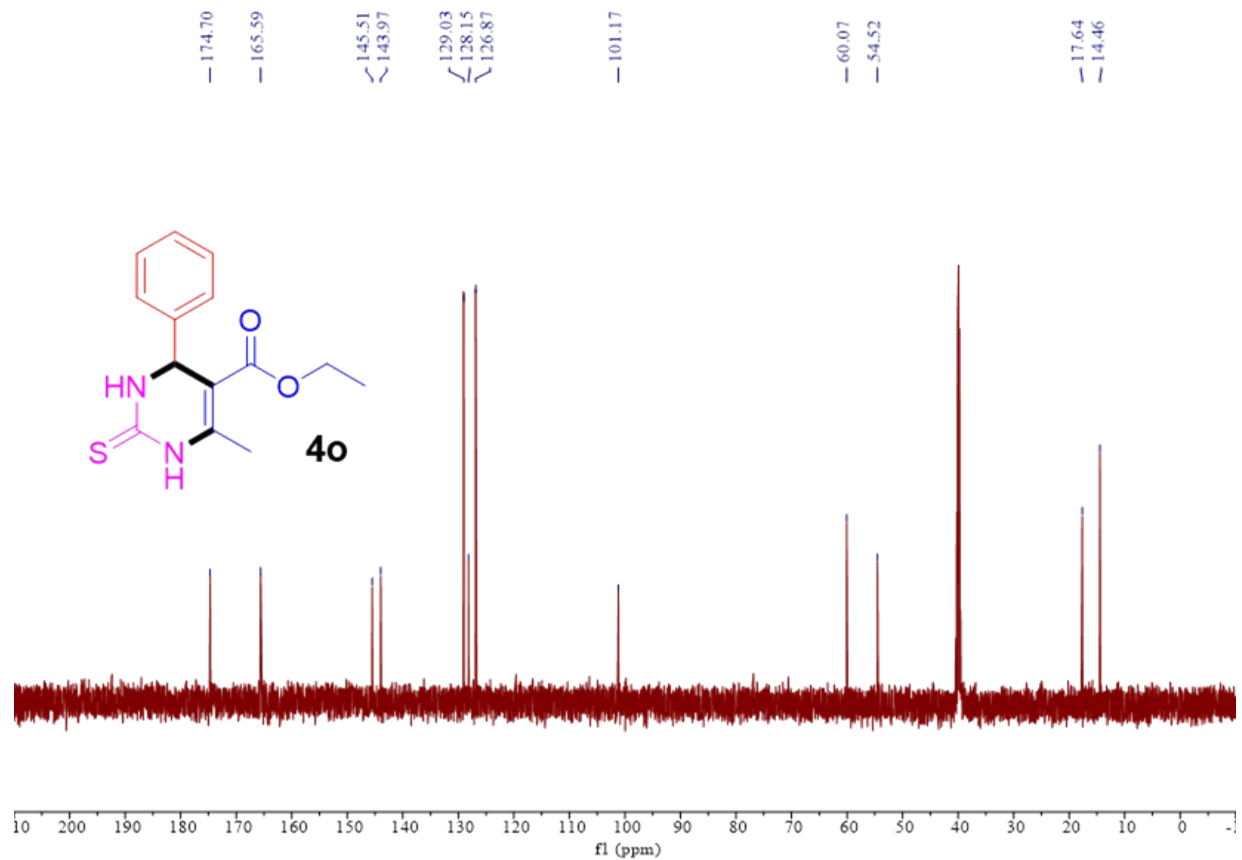
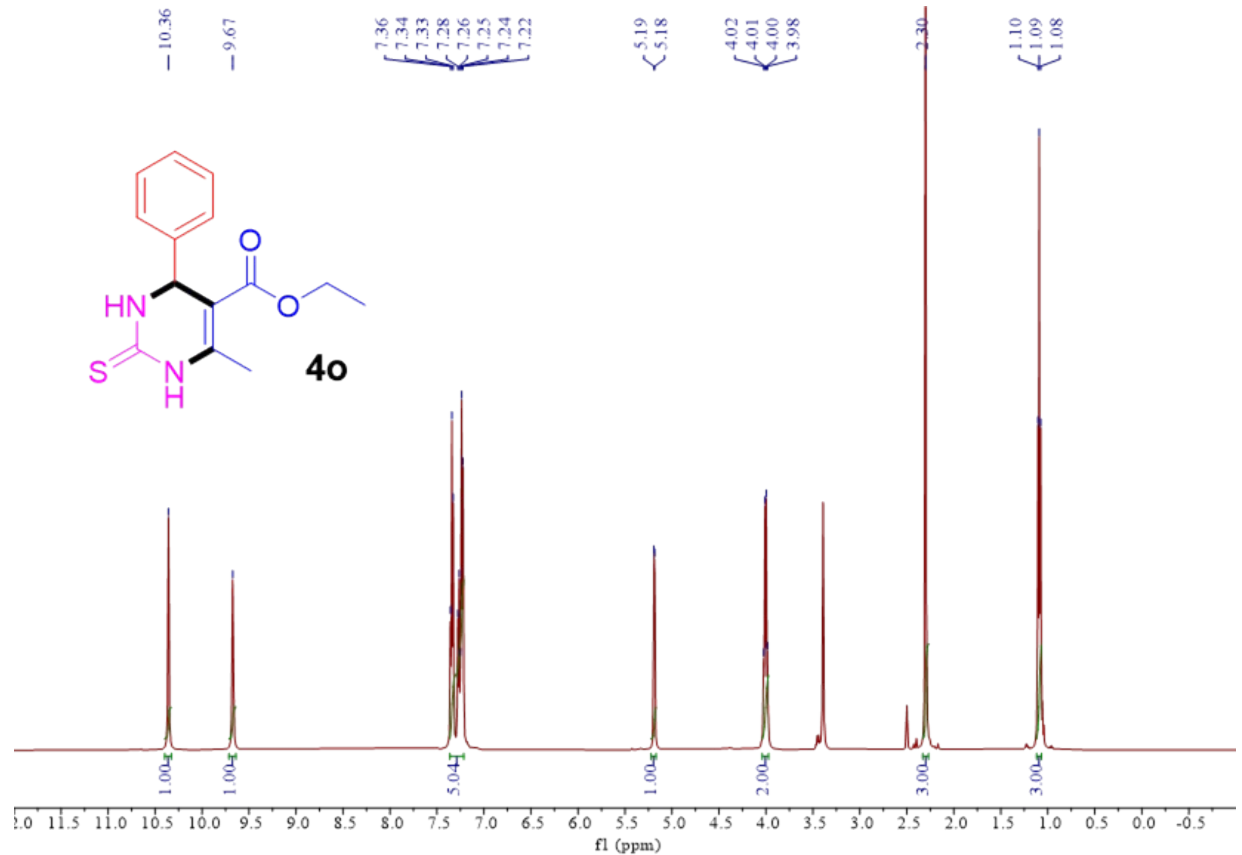












6. References

- 1 A. Tézé, G. Hervé, R. G. Finke and D. K. Lyon, α -, β -, and γ -Dodecatungstosilicic acids: isomers and related lacunary compounds. *Inorg Synth.* **1990**, *27*, 85.
- 2 Bruker, A. X. S. Inc., *APEX3 Package, APEX3, SAINT and SADABS*, Madison, Wisconsin, USA, **2016**.
- 3 (a) O. V. Dolomanov, L. J. Bourhis, R. J. Gildea, J. A. K. Howard and H. Puschmann, *OLEX2*: A complete structure solution, refinement and analysis program. *J. Appl. Cryst.* **2009**, *42*, 339-341; (b) G. M. Sheldrick, *SHELXT*-Integrated space-group and crystal-structure determination. *Acta Cryst.* **2015**, *A71*, 3-8; (c) G. M. Sheldrick, Crystal structure refinement with *SHELXL*. *Acta Cryst.* **2015**, *C71*, 3-8. (d) A. L. Spek, Single-crystal structure validation with the program *PLATON*. *J. Appl. Cryst.*, **2003**, *36*, 7-11; (e) A. L. Spek, Structure validation in chemical crystallography. *Acta Cryst.*, **2009**, *D65*, 148-155; (f) A. L. Spek, What makes a crystal structure report valid? *Inorg. Chim. Acta*, **2018**, *470*, 232-237.
- 4 K. Li, X. L. Lin, K. Zeng, X. F. Gao, W. Cen, Y. F. Liu and G. P. Yang, Effect of Na(I)-H₂O clusters on self-assembly of sandwich-type U(VI)-containing silicotungstates and the efficient catalytic activity for the synthesis of substituted phenylsulfonyl-1*H*-pyrazoles, *Tungsten*, **2022**, *4*, 149-157.
- 5 (a) I. D. Brown and D. Altermatt, Bond-valence parameters obtained from a systematic analysis of the inorganic crystal structure database. *Acta Cryst.* **1985**, *B41*, 244-247. (b) N. E. Brese, and M. O'Keeffe, Bond-valence parameters for solids. *Acta Cryst.* **1991**, *B47*, 192-197.
- 6 J. Goura, A. Sundar, B. S. Bassil, G. Ćirić-Marjanović, D. Bajuk-Bogdanović and U. Kortz, Peroxouranyl-containing W₄₈ wheel: synthesis, structure, and detailed infrared and Raman spectroscopy study, *Inorg. Chem.*, **2020**, *59*, 16789-16794.
- 7 (a) A. J. Gaunt, I. May, R. Copping, A. I. Bhatt, D. Collison, O. D. Fox, K. T. Holman and M. T. Pope, A new structural family of heteropolytungstate lacunary complexes with the uranyl, UO₂²⁺, cation, *Dalton Trans.*, **2003**, 3009-3014. (b) K.-C. Kim, A. Gaunt and M. T. Pope, New heteropolytungstates incorporating dioxouranium(VI). Derivatives of α -[SiW₉O₃₄]¹⁰⁻, α -[AsW₉O₃₃]⁹⁻, γ -[SiW₁₀O₃₆]⁸⁻, and [As₄W₄₀O₁₄₀]²⁸⁻, *J. Cluster Sci.*, **2002**, *13*, 423-436; (c) B. T. McGrail, G. E. Sigmon, L. J. Jouffret, C. R. Andrews and P. C. Burns, Raman spectroscopic and ESI-MS characterization of uranyl peroxide cage clusters. *Inorg. Chem.*, **2014**, *53*, 1562-1569.
- 8 (a) M. Y. Cheng, H. Y. Wang, Y. F. Liu, J. W. Shi, M. Q. Zhou, W. X. Du, D. D. Zhang and G. P. Yang, Bouquet-like uranium-containing selenotungstate consisting of two different Keggin-/Anderson-type units with excellent photoluminescence quantum yield, *Chin. Chem. Lett.*, **2023**, *34*, 107209; (b) H. Y. Wang, X. Y. Zheng, L. S. Long, X. J. Kong and L. S. Zheng, Sandwich-type uranyl phosphate-polyoxometalate cluster exhibiting strong luminescence, *Inorg. Chem.*, **2021**, *60*, 6790-6795.
- 9 (a) B. J. Yao, W. X. Wu, L. G. Ding and Y. B. Dong, Sulfonic acid and ionic liquid functionalized covalent organic framework for efficient catalysis of the biginelli reaction. *J. Org. Chem.* **2021**, *86*, 3024-3032. (b) L. G. do Nascimento, I. M. Dias, G. B. M. de Souza and C. G. Alonso, Niobium oxides as heterogeneous catalysts for biginelli multicomponent reaction. *J. Org. Chem.* **2020**, *85*, 11170-11180.